Experimental and Modeling Study of the Oxidation of Benzene

I. DA COSTA, R. FOURNET, F. BILLAUD, F. BATTIN-LECLERC

Département de Chimie Physique des Réactions, UMR 7630 CNRS, INPL-ENSIC 1, *rue Grandville*, BP 451, 54001 N*ancy Cedex*, F*rance*

Received 16 September 2002; accepted 6 June 2003

DOI 10.1002/kin.10148

ABSTRACT: This paper describes an experimental and modeling study of the oxidation of benzene. The low-temperature oxidation was studied in a continuous flow stirred tank reactor with carbon-containing products analyzed by gas chromatography. The following experimental conditions were used: 923 K, 1 atm, fuel equivalence ratios from 1.9 to 3.6, concentrations of benzene from 4 to 4.5%, and residence times ranging from 1 to 10 s corresponding to benzene conversion yields from 6 to 45%. The ignition delays of benzene–oxygen–argon mixtures with fuel equivalence ratios from 1 to 3 were measured behind shock waves. Reflected shock waves permitted to obtain temperatures from 1230 to 1970 K and pressures from 6.5 to 9.5 atm.

A detailed mechanism has been proposed and allows us to reproduce satisfactorily our experimental results, as well as some data of the literature obtained in other conditions, such as in a plug flow reactor or in a laminar premixed flame. The main reaction paths have been determined for the four series of measurements by sensitivity and flux analyses. © 2003 Wiley Periodicals, Inc. Int J Chem Kinet 35: 503–524, 2003

INTRODUCTION

The use of fuels in engines leads to a very significant formation of toxics (e.g. carbon monoxide, aldehydes, butadiene, aromatics, soot) and air pollutants (e.g. sulfur oxides, nitrogen oxides, unburned hydrocarbons and oxygenates) that are responsible for acid rain and the increase of the ozone concentration in the low atmosphere. The control of the influence of the formulation of fuels on the formation of pollutants requires a fundamental approach based on predictive models enabling us to quantify the formation of by-products during the process of combustion. The complexity of the chemistry of combustion is such that detailed chemical kinetic models, involving a description of elementary reactions, are necessary to model the formation of the broad spectrum of products observed.

Fuels contain usually six main classes of organic compounds: paraffins, isoparaffins, olefins, naphthenes, aromatics (including polyaromatic compounds), and ethers. Commercial gasoline contains approximately 150 different molecules belonging to these six classes of organic compounds. Since the end of the last decade, a great number of experimental and theoretical studies made it possible to model the combustion of model molecules taken individually and to predict the formation of characteristic pollutants. Nevertheless, most studies concern paraffins and isoparaffins and to a lesser extent, olefins and ethers [1]. Currently, the experimental and theoretical studies are directed toward the two other families of organic compounds, with an obvious interest for aromatic compounds. These last compounds are present in significant amounts in gasolines (∼35%) and diesel fuels (∼30%) [2] and are

Correspondence to: F. Battin-Leclerc; e-mail: dcpr@ensic.inpl-nancy.fr.

responsible for the formation of particles, which are harmful for health. The reactions of benzene as the first aromatic ring are of importance in building up polyaromatic hydrocarbons (PAHs), which are considered to play a key role in the formation of soot particles.

Benzene is the smallest aromatic molecule and its oxidation has consequently been the subject of a number of experimental studies in various types of reactors (laminar premixed flames [3,4], shock tube [5], plug flow reactors [6,7], jet-stirred reactors [8,9], and in a flow reactor in the flue gas of a laminar flame of methane [10]). Several kinetic mechanisms [4,7,9,11–16] have also been proposed to model these experimental data. It is worth noting that all the experiments in reactors with no initial radicals pool [6–9] have been performed using a low concentration of benzene ($\leq$0.16%) and, consequently, with no noticeable conversion for a temperature lower than 1000 K. The double purpose of this paper is then

- to present new experimental data for the oxidation of benzene obtained both in a jet-stirred reactor at a concentration of benzene from 4 to 4.5% and a temperature of 923 K, and in a shock tube for temperatures between 1230 and 1970 K.
- to propose a mechanism able to model these experimental results, but also to reproduce data of the literature obtained in a flow reactor at 1100 K [6] and in a near-sooting flat low-pressure laminar flame [3].

EXPERIMENTAL STUDY OF THE OXIDATION OF BENZENE

Experimental Procedure

This experimental study has been performed by using two different devices: a jet-stirred reactor and a shock tube. Benzene (99.8% pure) was provided by Aldrich. Oxygen (99.5% pure) and argon and helium (both 99.995% pure) were supplied by Alphagaz-L'Air Liquide.

Jet-Stirred Reactor. Figure 1 presents a scheme of the apparatus. Experiments were carried out in a continuous jet-stirred reactor (internal volume 88 cm^3) [15] made of quartz and operated at constant temperature (923 K) and pressure (1 atm). Residence times ranged from 1 to 10 s. The heating of the reactor was achieved by means of electrically insulated resistors directly coiled around the vessel; temperature was measured by using a thermocouple located inside the reactor in a glass finger. To obtain a spatially homogeneous temperature inside the reactor, reactants were preheated at

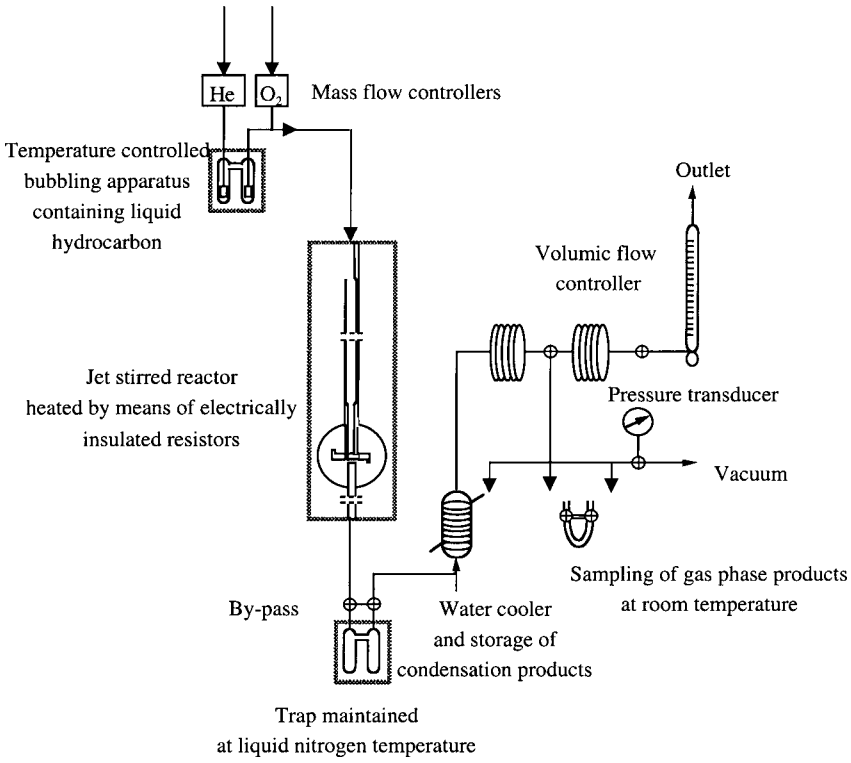

Figure 1 Scheme of the apparatus including a jet-stirred reactor.

a temperature close to the reaction temperature; corresponding residence time in the preheating section was approximately 1% of the total residence time. Temperature gradients inside the reactor, when reaction was occurring, were never larger than 5 K.

Gas-phase benzene was obtained by bubbling the flow of carrier gas (helium) into liquid benzene maintained at a temperature below room temperature (here at 280 K) to avoid the condensation of hydrocarbon before entering the reactor. Gas flows of helium and oxygen were measured by mass flow controllers; the gas flow of benzene was deduced from chromatography analyses. The benzene–helium–oxygen mixtures were mixed prior to their introduction into the reactor.

Because of the formation of compounds, which were either gaseous or liquid at room temperature, the analyses of the products leaving the reactor were performed in two steps:

- First, during a determined period of time, the outlet flow was directed toward a trap maintained at liquid nitrogen temperature. The short line between the reactor and the trap was heated up to 423 K to minimize condensation problems (this temperature was low enough for the oxidation reaction to be stopped). At the end of this period, the trap was removed and, after the addition of acetone and of an internal standard (*o*-xylene), progressively heated up at room so as temperature so as to melt its solid content. The obtained solution was then analyzed by gas chromatography with mass spectrometer or flame ionization detection by using a HP PONA capillary column and helium or nitrogen as carrier gas. In the conditions of this study, the column provided a good separation for the following products (with their measured retention time in minutes): benzene (8.9), toluene (12.1), ethyl benzene (15.5), *para*-xylene (15.9), styrene (16.5), benzaldehyde (18.7), phenol (19.2), benzylalcohol (20.5), and bibenzyl (31.1), with a limit of detection around 10^{-5} in mole fraction. Calibrations were performed by analyzing a range of solutions containing known amounts of *o*-xylene and of the compound to quantify.
- In a second time, just before the removal of the trap, the outlet flow was directed toward a water cooler and a volumic flowmeter. Gas samples were directly obtained by expansion in an evacuated volume. Chromatographs with thermal conductivity detector and hydrogen as carrier gas were used to analyze O_2, CO, and CO_2 with a Carbosphere packed column. Gas-phase light hydrocarbons (CH_4, C_2 species, C_3H_6, C_3H_6, and C_4H_6) were analyzed on a 30% Squalane on Chromosorb P column with detection by flame ionization detection and nitrogen as carrier gas. The analysis of water, hydrogen, methanol, and formaldehyde was not possible with our apparatuses. Calibrations were performed by analyzing a range of samples containing known pressures of each pure compound to quantify.

The compositions of the reacting flow were helium/oxygen/benzene = 80.5:15.5:4 (equivalence ratio $\Phi = 1.9$) and 96.1:9.4:4.5 ($\Phi = 3.6$) (mole). The equivalence ratio Φ is defined as $\Phi = 7.5 \times$ (%benzene/%oxygen) by using as a reference the total reaction

$$C_6H_6 + 7.5O_2 = 6CO_2 + 3H_2O$$

To check the initial mixture compositions, a complete cycle of analyses was performed, before each experiment, with the reactant gases circulating into the reactor at room temperature.

Shock Tube. As it is already described in detail in previous papers [17–19], we will just recall here the main features of this experimental device. The reaction (400 cm long, 7.8 cm i.d.) and the driver (90 cm long, 12.8 cm i.d.) parts of this stainless steel shock tube were separated by two terphane diaphragms, which were ruptured by decreasing suddenly the pressure in the space separating them. The driver gas was helium. The incident and reflected shock velocities were measured by four piezoelectric pressure transducers located along the reaction section. The temperature and the pressure of the test gas behind the incident and the reflected shock waves were derived from the value of the incident shock velocity by using ideal one-dimensional shock equations.

The onset of ignition was detected by OH radical emission at 306 nm through a quartz window with a photomultiplier fitted with a monochromator at the end of the reaction part. The last pressure transducer was located at the same place along the axis of the tube as the quartz window. The ignition delay time was defined as the time interval between the pressure rise measured by the last pressure transducer owing to the arrival of the reflected shock wave and the rise of the optical signal by the photomultiplier up to 10% of its maximum value.

Fresh reaction mixtures were manometrically prepared every day and mixed using a recirculation pump. Before each introduction of the reaction mixture (from 100 to 400 kPa), the reaction section was flushed with

pure argon and evacuated (below 10^{-2} kPa), so that the residual gas was mainly argon.

Experimental Results

A discussion of these experimental results is given further in the text with the comparisons with simulations.

Jet-Stirred Reactor. The main carbon-containing products analyzed by gas chromatography were phenol, carbon monoxide and dioxide, methane, C_2 species (acetylene and ethylene were not separated), propyne, propene, and 1,3-butadiene. For each sample, the carbon balance was checked and an agreement was obtained to within 5%. The formation of cyclopentadiene was too low to be detected.

Table I presents the experimental results obtained in a jet-stirred reactor. Figures 2 and 3 display the evolution of the conversions of benzene and oxygen and of the formations of product vs. residence time for equivalence ratios equal to 1.9 and 3.6, respectively. A decrease of the equivalence ratio of the mixtures enhances the rate of consumption of benzene, but does not really change the repartition of the observed product, except carbon monoxide, which is formed in higher concentration at Φ equal to 1.9.

Shock Tube. This study was performed in the following experimental conditions (after the reflected shock):

- Temperature (T) range from 1230 to 1970 K.
- Pressure (P) range from 7.3 to 9.5 atm.
- Argon–benzene–oxygen mixtures (in molar percent) were 1.25:18.75:80, 1.25:9.375:89.375, 1.25:6.26:92.49, 1.25:3.125:95.625, and 2.5:18.75:78.75, respectively, which correspond to four different equivalence ratios ($\Phi = 0.5$, 1, 1.5, and 3) and to two different concentrations of benzene (1.25 and 2.5%) and permit to obtain corresponding delays from 6 to 1980 μs.

Table II and Fig. 4 present the experimental data thus obtained.

For the five mixtures, ignition delays (τ) decrease when T rises up and varies exponentially vs. 1000/T. It is also shown that for a given T, ignition delays decrease with the equivalence ratio of the mixture for a given concentration of benzene and with the concentration of hydrocarbon for a given equivalence ratio. The slope of the log (τ) vs. 1000/T lines remains nearly constant when the equivalence ratio varies, but decreases with the concentration of benzene. The lower part of Fig. 4 also presents the line obtained from the correlation proposed by Burcat et al. [5], $\tau = 1.26 \times 10^{-15}$

Table I Experimental Results Obtained in a Jet-Stirred Reactor at 923 K and 1 atm

	Mole Fractions at Different Residence Times (s)						
Compounds	1.6	2.2	3.3	4.4	5.5	6.6	8.8
(A) $\phi = 1.9$; $X_{benzene} = 0.04$							
CH_4	1.34×10^{-6}	2.57×10^{-6}	1.15×10^{-4}	2.79×10^{-4}	5.57×10^{-4}	7.77×10^{-4}	1.0×10^{-3}
$C_2H_2 + C_2H_4$	1.48×10^{-6}	3.39×10^{-6}	1.8×10^{-4}	3.16×10^{-4}	5.46×10^{-4}	6.74×10^{-4}	7.9×10^{-4}
C_3H_4	1.98×10^{-7}	3.93×10^{-7}	8.11×10^{-6}	7.72×10^{-6}	7.78×10^{-6}	8.17×10^{-6}	8.74×10^{-6}
C_3H_6	2.2×10^{-7}	6.24×10^{-7}	1.61×10^{-5}	2.46×10^{-5}	3.97×10^{-5}	4.26×10^{-5}	4.84×10^{-5}
1,3-C_4H_6	0	0	2.97×10^{-6}	8.23×10^{-6}	8.43×10^{-6}	1.23×10^{-5}	1.55×10^{-5}
O_2	0.155	0.155	0.148	0.134	0.127	0.114	0.112
CO	0	0	1.69×10^{-2}	2.94×10^{-2}	4.66×10^{-2}	5.58×10^{-2}	6.6×10^{-2}
CO_2	0	0	1.68×10^{-3}	5.17×10^{-3}	5.61×10^{-3}	8.85×10^{-3}	6.3×10^{-3}
C_6H_6	*0.0375*	*0.0338*	*0.0322*	*0.0305*	*0.0227*	*0.0232*	*0.0221*
C_6H_5OH	0	0	1.03×10^{-3}	1.81×10^{-3}	1.69×10^{-3}	1.87×10^{-3}	1.72×10^{-3}
(B) $\phi = 3.6$; $X_{benzene} = 0.045$							
CH_4	2.28×10^{-6}	2.59×10^{-6}	1.77×10^{-5}	8.84×10^{-5}	2.37×10^{-4}	4.32×10^{-4}	6.23×10^{-4}
$C_2H_2 + C_2H_4$	9.71×10^{-7}	1.6×10^{-6}	2.4×10^{-5}	1.42×10^{-4}	3.02×10^{-4}	4.79×10^{-4}	6.02×10^{-4}
C_3H_4	0	0	1.62×10^{-6}	4.34×10^{-6}	5.32×10^{-6}	5.63×10^{-6}	5.92×10^{-6}
C_3H_6	0	0	3.41×10^{-6}	8.66×10^{-6}	1.65×10^{-5}	3.46×10^{-5}	3.99×10^{-5}
1,3-C_4H_6	0	0	1.99×10^{-6}	5.35×10^{-6}	6.79×10^{-6}	1.32×10^{-5}	1.77×10^{-5}
O_2	0.0921	0.0897	0.0803	0.076	0.08	0.07	0.0629
CO	0	0	0	1.06×10^{-2}	1.98×10^{-2}	2.57×10^{-2}	3.62×10^{-2}
CO_2	0	0	0	1.13×10^{-3}	3.22×10^{-3}	2.8×10^{-3}	9.28×10^{-3}
C_6H_6	*0.042*	*0.0397*	*0.0349*	*0.0361*	*0.035*	*0.0325*	*0.0287*
C_6H_5OH	0	0	2.77×10^{-5}	8.61×10^{-4}	1.35×10^{-3}	1.56×10^{-3}	1.4×10^{-3}

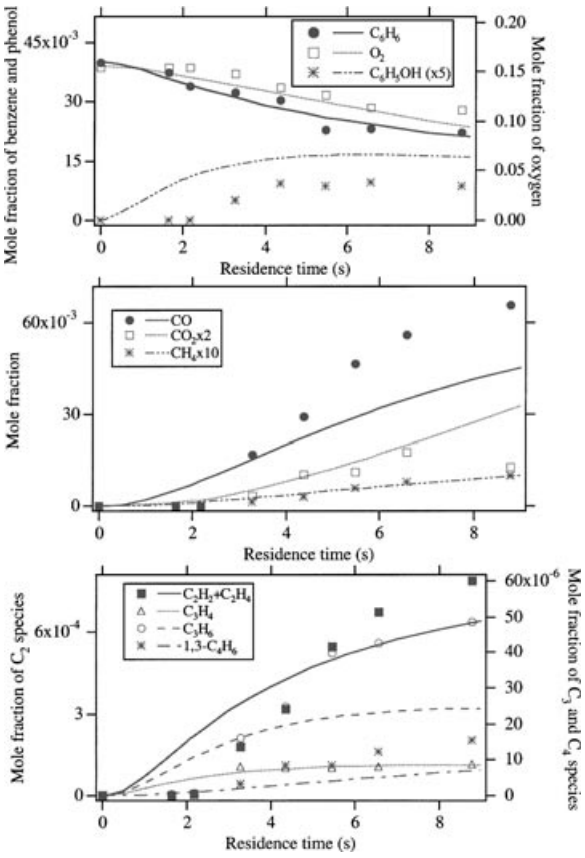

Figure 2 Oxidation of benzene in a jet-stirred reactor at 923 K. Comparison between experimental (symbols) and computed (lines) species vs. residence time at $\Phi = 1.9$.

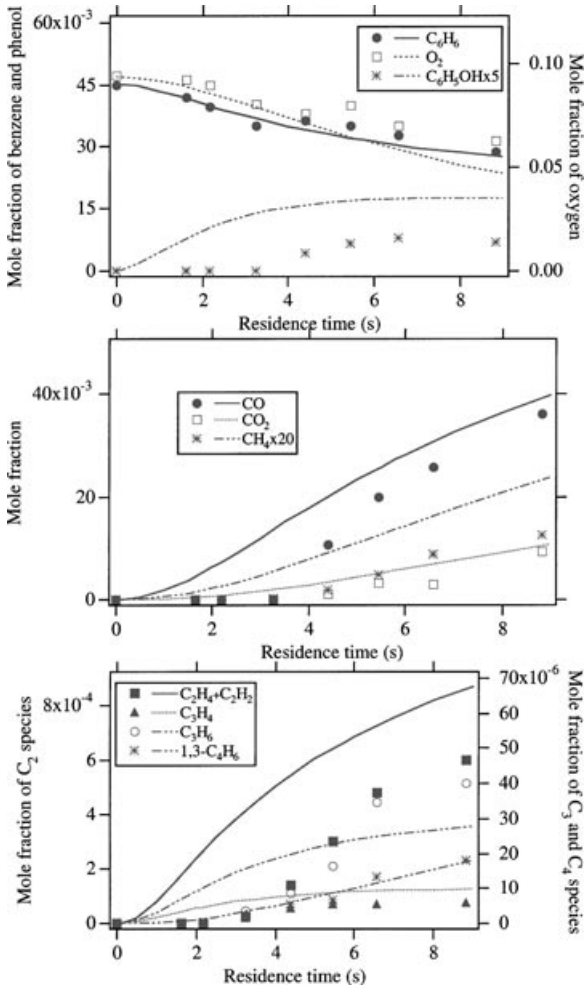

Figure 3 Oxidation of benzene in a jet-stirred reactor at 923 K. Comparison between experimental (symbols) and computed (lines) species vs. residence time at $\Phi = 3.6$.

$\times$ exp(40.6 kcal mol^{-1}/RT) $\times$ $[C_6H_6]^{0.42}$ $\times$ $[O_2]^{-1.70}$ $\times$ $[Ar]^{0.44}$ s (concentrations in mol cm^{-3} units), based on their experimental results, at $\Phi = 1$ and at 1.25% of benzene.

DESCRIPTION OF THE REACTION MECHANISM

This mechanism, which is available on request, has been written in the CHEMKIN II [20] format and includes three parts:

- The C_0–C_6 reaction base, which is described in recent papers [18,19]. This C_0–C_6 reaction base was built from a review of the recent literature and is an extension of our previous C_0–C_2 reaction base [21]. This C_0–C_2 reaction base includes the reactions of radicals or molecules including carbon, hydrogen, and oxygen atoms and containing less than three carbon atoms. The kinetic data used in this base were taken from the literature and are mainly those proposed by Baulch et al. [22] and Tsang and Hampson [23]. The C_0–C_2 reaction base was first presented in the paper of Barbé et al. [21] and has been updated recently [19]. The C_0–C_6 reaction base includes reactions involving C_3H_2··, ·C_3H_3, C_3H_4 (allene and propyne), ·C_3H_5 (three isomers), C_3H_6, C_4H_2, ·C_4H_3 (2 isomers), C_4H_4, ·C_4H_5 (5 isomers), C_4H_6 (1,3-butadiene, 1,2-butadiene, methylcyclopropene, 1-butyne, and 2-butyne), as well as the formation of benzene [18,19]. Pressure-dependent rate constants follow the formalism proposed by Troe [24] and efficiency coefficients have been included. This reaction base was built in order to model experimental results obtained in a jet-stirred reactor for methane and ethane [21], profiles in laminar flames of methane, acetylene,

Table II Mixture Compositions, Shock Conditions, and Ignition Delays for Benzene

Composition (Mole Percent)		P_1	V	P_5	T_5	τ	Composition (Mole Percent)		P_1	V	P_5	T_5	τ
C_6H_6	O_2	(atm)	(m s^{-1})	(atm)	(K)	(μs)	C_6H_6	O_2	(atm)	(m s^{-1})	(atm)	(K)	(μs)
1.25	9.375	0.2105	875	8.57	1579	8	2.5	18.75	0.2237	852	9.11	1362	29
		0.2105	874	8.52	1573	15			0.2303	830	8.69	1306	80
$\phi = 1$		0.2039	862	7.93	1536	15	$\phi = 1$		0.2368	825	8.77	1293	167
		0.2368	849	8.84	1498	34			0.2434	829	9.15	1304	171
		0.2105	847	7.80	1491	35			0.2637	818	9.51	1277	263
		0.2237	849	8.36	1500	35			0.2632	808	9.17	1254	563
		0.2500	835	8.89	1456	70			0.2526	799	8.50	1231	1167
		0.2633	803	8.35	1361	99			0.2763	802	9.40	1238	840
		0.2704	820	9.14	1411	124							
		0.2633	813	8.69	1391	131	1.25	6.25	0.1908	892	8.13	1659	10
		0.2763	799	8.65	1351	198			0.2276	865	8.43	1572	31
		0.2568	813	8.46	1390	200			0.2237	849	8.50	1523	75
		0.2829	806	9.11	1372	203	$\phi = 1.5$		0.2039	844	7.46	1511	66
		0.2763	802	8.76	1359	283			0.1974	805	6.28	1391	229
		0.3033	792	9.27	1332	301			0.2368	821	8.17	1436	215
		0.2895	782	8.52	1304	357			0.2171	830	7.57	1468	110
		0.2961	790	8.99	1326	503			0.2309	827	7.97	1459	125
		0.2907	783	8.59	1305	543			0.1980	817	6.59	1428	152
		0.3166	782	9.30	1303	1978			0.1842	871	7.35	1593	39
1.25	18.75	0.2251	847	8.44	1418	17	1.25	3.125	0.1447	972	7.78	1970	6
		0.2434	847	9.13	1418	23			0.1513	951	7.65	1893	8.5
$\phi = 0.5$		0.2237	847	8.39	1418	31	$\phi = 3$		0.1579	923	7.36	1797	15
		0.2368	839	8.61	1394	42							
		0.2500	806	8.09	1304	46							
		0.2566	815	8.58	1328	60							
		0.2105	831	7.45	1372	86							
		0.2829	814	9.43	1326	111							
		0.2763	816	9.29	1332	151							
		0.2697	804	8.69	1301	168							
		0.2632	800	8.35	1290	257							

Note. P_1 is the pressure of the mixture before the shock, V the speed of the incident wave, P_5 and T_5 are pressure and temperature behind the reflected shock wave, and τ is the ignition delay time.

and 1,3-butadiene [18], and shock tube autoignition delays for acetylene, propyne, allene, 1,3-butadiene [18], 1-butyne, and 2-butyne [19].

- A primary mechanism containing 71 reactions, in which only benzene and oxygen were considered as molecular reactants.
- A secondary mechanism including 64 reactions, in which the reactants are the molecular products formed by the primary mechanism.

When it was possible, specific heats, heats of formation, and entropies of the considered molecules or radicals have been calculated using the software THERGAS [25], based on the group and bond additivity methods proposed by Benson [26], and stored as 14 polynomial coefficients, according to the CHEMKIN II formalism [20]. In the case of the thermochemistry of cyclopentadienone, cyclopentadienol and orthobenzoquinone molecules and of cyclopentadienonyl, cyclopentadienoxy, and hydroxycyclopentadienyl radicals, for which the calculation was not possible by THERGAS, because some groups were missing, polynomial coefficients have been derived from the thermochemical data proposed by Alzueta et al. [7]. The groups responsible for failing in applying THERGAS are CO─(CO)─(Cd), CO─(Cd)─(CO), CO─(Cd)─(Cd), and C─(Cd)/2─(h)─(O). In the future, these groups should be calculated by means of thermodynamic data found in the literature [7] and included in the software. It is worth noting that, in the distributed version of THERGAS, the introduction of new groups required to modify some data files, which are not accessible by the user. Table III presents the heats of formation used for aromatic species. It must

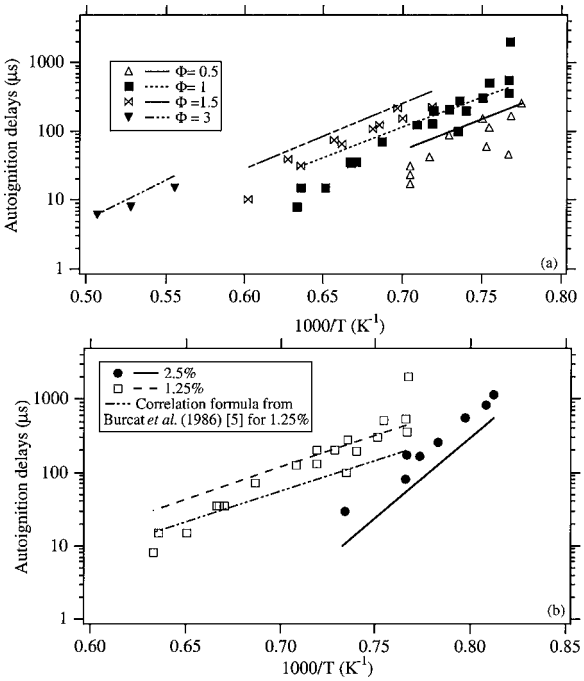

Figure 4 Autoignition delays of benzene in a shock tube. Semilog plot of experimental (symbols) and computed (lines) ignition delays as a function of temperature behind the reflected shock wave for different equivalence ratios at 1.25% of benzene (a) and for different benzene concentrations at $\Phi = 1$ (b). The correlation proposed by Burcat et al. [5] at $\Phi = 1$ and at 1.25% of benzene is shown in (b).

be kept in mind that the precision obtained by using group additivity methods to estimate heats of formation is around 2 kcal mol^{-1} for molecules and 4 kcal mol^{-1} for radicals [26].

Table III Heats of Formation for Aromatic Species at 298 K in kcal mol^{-1}

Species	ΔH_f (298 K)
C_6H_6	19.8
C_6H_5OH	−23.1
C_5H_6	32
C_5H_5OH*	−9
C_5H_4O*	13.2
C_6H_5OO	31
C_6H_5	81
C_6H_5O	12.8
C_5H_5	61
C_5H_4OH*	15.9
C_5H_3O*	67
OC_6H_4O*	−25

Note. The heats of formation have been calculated by the software THERGAS [25], except for the compounds distinguished by "*", for which they have been proposed by Alzueta et al. [7].

The primary and secondary mechanisms for the oxidation of benzene are presented in Table IV, as well as the references related to the used kinetic data. These mechanisms, which involve 24 species not included in the C_0—C_6 reaction base, have been built in order to be more comprehensive than those proposed by Emdee et al. [12] and Alzueta et al. [7] to model experimental results around 1000 K, e.g., termination steps of resonance-stabilized radicals have been considered in more details.

Primary Mechanism

The primary mechanism includes the reactions of benzene molecules and of cyclohexadienyl, phenyl, phenylperoxy, phenoxy, hydroxyphenoxy, cyclopentadienyl, cyclopentadienoxy, and hydroxycyclopentadienyl free radicals.

Reactions of benzene molecules involve the formation of phenyl radicals by unimolecular (1) (reaction numbers are those of Table IV) and bimolecular (2) initiations and by metatheses with H-abstraction by ·H (8), ·O· (9), ·OH (10), $\cdot HO_2$ (11), $\cdot CH_3$ (12), $\cdot C_2H_5$ (13), $\cdot a\text{-}C_3H_5$ (14), $\cdot n\text{-}C_4H_5$ (14), and $\cdot i\text{-}C_4H_5$ (16) radicals. Addition reactions are also considered to form $\cdot C_6H_7$ radicals (addition of ·H atoms (3)), phenoxy radicals (addition of ·O· atoms (4)), phenol (addition of ·OH radicals (5)), phenylacetylene (addition of $\cdot C_2H$ radicals (6)), and styrene (addition of $\cdot C_2H_3$ radicals (7)). The decomposition of benzene molecule to give propargyl radicals is already included in the C_0—C_6 reaction base through its reverse reaction. The kinetic value and the products of the combination of propargyl radicals is still a subject of discussion [51]. In the C_0—C_6 reaction base, we have considered the formation of benzene with a rate constant $k = 1 \times 10^{12}$ cm^3 s^{-1} mol^{-1} close to the value estimated by Stein et al. [52] (3×10^{12} cm^3 s^{-1} mol^{-1}). Recent measurements [51] proposed a rate between 4.5×10^{12} and 9×10^{12} $cm^3 s^{-1} mol^{-1}$ for the formation of linear and cyclic C_6H_6 and found that the contribution of the formation of phenyl radicals and H· atoms was less than 10%.

Reactions of resonance-stabilized cyclohexadienyl radicals include their linearization (17) as proposed by Weissman and Benson [32], their oxidation with O_2 (18) as usual allylic radicals, and their termination reactions with other radicals (20–23). Their decomposition by beta-scission to produce acetylene and $\cdot n\text{-}C_4H_5$ radicals is already considered in the C_0—C_6 reaction base (written in the reverse direction).

The linearization of phenyl radicals (24) has been considered as proposed by Braun-Unkoff et al. [33]. The rate constants of the decomposition reactions of the linear $\cdot C_6H_5$ isomer (25–26) have been reevaluated in

Table IV Primary and Secondary Mechanisms for the Oxidation of Benzene

Reactions	A	n	E_a	References	Reaction No.
PRIMARY MECHANISM					
Reactions of benzene molecules					
Umimolecular initiation					
$C_6H_5 + H(+M) \leftrightharpoons C_6H_6(+M)$					
k_∞	1.0×10^{14}	0.0	0.0	Wang [27]	(1)
k_0	6.6×10^{75}	−16.3	7.0		
Troe's factors: 1.0, 0.1, 585, 6113					
Efficiency factors: O_2, 0.4; CO, 0.75; CO_2, 1.5; H_2O, 6.5; N_2, .4; Ar, 0.35; He, 0.35; C_6H_6, 3.0					
Bimolecular initiation					
$C_6H_6 + O_2 \leftrightharpoons C_6H_5 + HO_2$	6.0×10^{13}	0.0	63.4	Alzueta [7]	(2)
Additions					
$C_6H_6 + H \leftrightharpoons C_6H_7$	3.2×10^{13}	0.0	3.2	Mebel [28]	(3)
$C_6H_6 + O \leftrightharpoons C_6H_5O + H$	2.8×10^{13}	0.0	4.9	Nicovich [29]	(4)
$C_6H_6 + OH \times C_6H_5OH + H$	1.3×10^{13}	0.0	10.6	Baulch [22]	(5)
$C_6H_6 + C_2H \leftrightharpoons C_6H_5C_2H + H$	5.0×10^{13}	0.0	0.0	Wang [27]	(6)
$C_6H_6 + C_2H_3 \leftrightharpoons$ styrene + H	7.9×10^{11}	0.0	6.4	Wang [27]	(7)
Metatheses					
$C_6H_6 + H \leftrightharpoons C_6H_5 + H_2$	6.0×10^{8}	1.0	16.8	Mebel [28]	(8)
$C_6H_6 + O \leftrightharpoons C_6H_5 + OH$	2.0×10^{13}	0.0	14.7	Lindstedt [13]	(9)
$C_6H_6 + OH \leftrightharpoons C_6H_5 + H_2O$	1.6×10^{8}	1.42	1.45	Baulch [30]	(10)
$C_6H_6 + HO_2 \leftrightharpoons C_6H_5 + H_2O_2$	5.5×10^{12}	0.0	28.9	Baulch [22]	(11)
$C_6H_6 + CH_3 \leftrightharpoons C_6H_5 + CH_4$	2.0×10^{12}	0.0	15.0	Zhang [31]	(12)
$C_6H_6 + C_2H_5 \leftrightharpoons C_6H_5 + C_2H_6$	6.3×10^{11}	0.0	15.0	Zhang [31]	(13)
$C_6H_6 + a\text{-}C_3H_5 \leftrightharpoons C_6H_5 + C_3H_6$	6.3×10^{11}	0.0	20.0	Estimated[a]	(14)
$C_6H_6 + n\text{-}C_4H_5 \leftrightharpoons C_6H_5 + 1,3\text{-}C_4H_6$	6.3×10^{11}	0.0	15.0	Estimated[a]	(15)
$C_6H_6 + i\text{-}C_4H_5 \leftrightharpoons C_6H_5 + 1,3\text{-}C_4H_6$	6.3×10^{11}	0.0	20.0	Estimated[a]	(16)
Reactions of cyclohexadienyl radicals (resonance-stabilized)					
Isomerization					
$C_6H_7 \leftrightharpoons l\text{-}C_6H_7$	2.5×10^{14}	0.7	41.8	Weissman [32]	(17)
Oxidation					
$C_6H_7 + O_2 \leftrightharpoons C_6H_6 + HO_2$	7.9×10^{11}	0.0	9.9	Estimated[b]	(18)
Combinations					
$C_6H_7 + H \leftrightharpoons C_6H_8$	1.0×10^{14}	0.0	0.0	Estimated[c]	(19)
Disproportionations					
$C_6H_7 + H \leftrightharpoons C_6H_6 + H_2$	3.3×10^{12}	0.0	0.0	Ristori [9]	(20)
$C_6H_7 + OH \leftrightharpoons C_6H_6 + H_2O$	1.0×10^{13}	0.0	0.0	Estimated[d]	(21)
$C_6H_7 + CH_3 \leftrightharpoons C_6H_6 + CH_4$	3.0×10^{12}	−0.32	−0.1	Estimated[d]	(22)
$C_6H_7 + C_6H_7 \leftrightharpoons C_6H_6 + C_6H_8$	8.4×10^{10}	0.0	−0.3	Estimated[d]	(23)
Reactions of phenyl radicals					
Isomerization and decompositions by beta-scission					
$C_6H_5 \leftrightharpoons l\text{-}C_6H_5$	5.0×10^{13}	0.0	72.5	Braun-Unkhoff [33]	(24)
$l\text{-}C_6H_5 \leftrightharpoons C_2H_2 + C_4H_3$	2.0×10^{13}	0.0	51.0	Estimated[e]	(25)
$l\text{-}C_6H_5 \leftrightharpoons l\text{-}C_6H_4 + H$	2.0×10^{12}	0.0	41.0	Estimated[e]	(26)
Reactions with O_2					
$C_6H_5 + O_2 \leftrightharpoons C_6H_5O + O$	2.6×10^{13}	0.0	6.1	Frank [34]	(27)
$C_6H_5 + O_2 \leftrightharpoons OC_6H_4O + H$	3.0×10^{13}	0.0	9.0	Frank [34]	(28)
$C_6H_5 + O_2 \leftrightharpoons C_6H_5O_2$	2.2×10^{19}	−2.5	0.0	Estimated[f]	(29)
Additions					
$C_6H_5 + C_2H_2 \leftrightharpoons C_6H_5C_2H + H$	4.0×10^{13}	0.0	10.1	Marinov [35]	(30)
$C_6H_5 + C_6H_6$ biphenyl + H	5.6×10^{12}	−0.074	7.5	Wang [27]	(31)
Combinations (followed in some cases by decompositions)					
$C_6H_5 + O \leftrightharpoons C_5H_5 + CO$	1.0×10^{14}	0.0	0.0	Frank [34]	(32)
$C_6H_5 + OH \leftrightharpoons C_6H_5OH$	1.0×10^{13}	0.0	0.0	Calculated[g]	(33)
Toluene $\leftrightharpoons C_6H_5 + CH_3$	1.0×10^{16}	0.0	97.0	Colket [36]	(34)
$C_6H_5 + CHO \leftrightharpoons C_6H_5CHO$	5.0×10^{12}	0.0	0.0	Calculated[g]	(35)

Continued

Table IV Continued

Reactions	A	n	E_a	References	Reaction No.
$C_6H_5 + C_2H_3 \leftrightharpoons$ styrene	5.0×10^{12}	0.0	0.0	Calculated[g]	(36)
$C_6H_5 + C_2H_5 \leftrightharpoons$ ethylbenzene	5.0×10^{12}	0.0	0.0	Calculated[g]	(37)
$C_6H_5 + HO_2 \leftrightharpoons C_6H_5O + OH$	5.0×10^{12}	0.0	0.0	Calculated[g]	(38)
$C_6H_5 + C_3H_3 \leftrightharpoons C_6H_5C_3H_3$	3.0×10^{12}	0.0	0.0	D'Anna [37]	(39)
$C_6H_5 + C_6H_5 \leftrightharpoons$ biphenyl	3.8×10^{31}	−5.75	7.9	Wang [27]	(40)
Disproportionations					
$C_6H_5 + OH \leftrightharpoons C_6H_5O + H$	5.0×10^{13}	0.0	0.0	Alzueta [7]	(41)
$C_6H_5 + C_6H_7 \leftrightharpoons C_6H_6 + C_6H_6$	1.0×10^{12}	0.0	0.0	Shandross [4]	(42)
Reactions of peroxyphenyl radicals					
Decomposition by beta-scission					
$C_6H_5O_2 \leftrightharpoons OC_6H_4O + H$	2.0×10^{13}	0.0	30.0	Estimated[h]	(43)
$C_6H_5O_2 \leftrightharpoons C_5H_4O + CHO$	2.0×10^{13}	0.0	30.0	Estimated[h]	(44)
Reactions of phenoxy radicals (resonance-stabilized)					
CO elimination					
$C_6H_5O \leftrightharpoons CO + C_5H_5$	2.5×10^{11}	0.0	43.8	Baulch [30]	(45)
Terminations					
$C_6H_5O + H(+M) \leftrightharpoons C_6H_5OH(+M)$					
k_∞	1.0×10^{14}	0.0	0.0	Estimated[c]	(46)
k_0	1.0×10^{94}	−21.84	13.9	Wang [27]	
Troe's factors: 0.043, 304, 60000, 5896					
Efficiency factors: O_2, 0.4; CO, 0.75; CO_2, 1.5; H_2O, 6.5; N_2, .4; Ar, 0.35; He, 0.35; C_6H_6, 3.0					
$C_6H_5O + H \leftrightharpoons C_5H_6 + CO$	1.1×10^{53}	−10.7	41.4	Tan [15]	(47)
$C_6H_5O + O \leftrightharpoons OC_6H_4OH$	2.6×10^{10}	0.47	0.8	Lin [38]	(48)
$C_6H_5O + O \leftrightharpoons OC_6H_4O + H$	8.5×10^{13}	0.0	0.0	Alzueta [7]	(49)
$C_6H_5O + O \leftrightharpoons C_5H_5 + CO_2$	1.0×10^{13}	0.0	0.0	Alzueta [7]	(50)
Reactions of $HOC_6H_4O\cdot$ radicals (resonance-stabilized)					
CO elimination					
$OC_6H_4OH \leftrightharpoons CO + C_5H_4OH$	7.4×10^{11}	0.0	43.8	Estimated[i]	(51)
Reactions of cyclopentadienyl radicals (resonance-stabilized)					
Isomerization and decompositions by beta-scission					
$C_5H_5 \leftrightharpoons l\text{-}C_5H_5$	1.0×10^{14}	0.0	45.5	Braun [33]	(52)
$l\text{-}C_5H_5 + H \leftrightharpoons l\text{-}C_5H_6$	1.0×10^{14}	0.0	0.0	Estimated[c]	(53)
$l\text{-}C_5H_5 \leftrightharpoons C_3H_3 + C_2H_2$	2.0×10^{13}	0.0	50.0	Estimated[e]	(54)
Reactions with O_2					
$C_5H_5 + O_2 \leftrightharpoons CHO + C_4H_4O$	1.2×10^{19}	−2.48	11.0	Zhong [39]	(55)
Combinations					
$C_5H_5 + H \leftrightharpoons C_5H_6$	1.0×10^{14}	0.0	0.0	Estimated[c]	(56)
$C_5H_5 + O \leftrightharpoons C_5H_4O + H$	5.8×10^{13}	−0.02	0.02	Zhong [39]	(57)
$C_5H_5 + O \leftrightharpoons 2C_2H_2 + CHO$	3.2×10^{13}	−0.17	0.44	Zhong [39]	(58)
$C_5H_5 + OH \leftrightharpoons C_5H_5OH$	1.0×10^{13}	0.0	0.0	Calculated[g]	(59)
$C_5H_5 + HO_2 \leftrightharpoons C_5H_5O + OH$	3.0×10^{12}	0.0	0.0	Calculated[g]	(60)
$C_5H_5 + C_5H_5 \leftrightharpoons C_{10}H_{10}$	2.0×10^{12}	0.0	0.0	Calculated[g]	(61)
Disproportionations					
$C_5H_5 + HO_2 \leftrightharpoons C_5H_6 + O_2$	2.5×10^{9}	1.0	3.5	Estimated[j]	(62)
Reactions of cyclopentadienoxy radicals					
Decompositions by beta-scission					
$C_5H_5O \leftrightharpoons 2C_2H_2 + CHO$	2.0×10^{13}	0.0	30.0	Estimated[k]	(63)
$C_5H_5O \leftrightharpoons C_5H_4O + H$	2.0×10^{13}	0.0	30.0	Estimated[k]	(64)
Combinations					
$C_5H_5O + H \leftrightharpoons C_5H_5OH$	1.0×10^{14}	0.0	0.0	Estimated[c]	(65)
Reactions of hydroxyclopentadienyl (resonance-stabilized)					
Oxidation					
$C_5H_4OH + O_2 \leftrightharpoons C_5H_4O + HO_2$	1.0×10^{13}	0.0	5.0	Estimated[l]	(66)
Combinations					
$C_5H_4OH + H \leftrightharpoons C_5H_5OH$	1.0×10^{14}	0.0	0.0	Estimated[c]	(67)

Continued

Table IV Continued

Reactions	A	n	E_a	References	Reaction No.
$C_5H_4OH + O \leftrightharpoons CO_2 + C_2H_2 + C_2H_3$	3.2×10^{13}	−0.17	0.44	Estimated[m]	(68)
$C_5H_4OH + HO_2 \leftrightharpoons OH + CO_2 + C_2H_3 + C_2H_2$	3.0×10^{12}	0.0	0.0	Estimated[m]	(69)
Disproportionations					
$C_5H_4OH + HO_2 \leftrightharpoons C_5H_5OH + O_2$	2.5×10^{9}	1.0	3.5	Estimated[m]	(70)
$C_5H_4OH + C_6H_5O \leftrightharpoons C_5H_4O + C_6H_5OH$	1.0×10^{12}	0.0	0.0	Estimated[n]	(71)
SECONDARY MECHANISM					
Reactions of ortho-benzoquinone molecules					
$OC_6H_4O \leftrightharpoons C_5H_4O + CO$	1.0×10^{12}	0.0	40.0	Frank [34]	(72)
$OC_6H_4O + H \leftrightharpoons 2CO + C_2H_2 + C_2H_3$	5.2×10^{13}	0.0	3.2	Estimated[o]	(74)
$OC_6H_4O + H \leftrightharpoons H_2 + 2CO + C_2H_2 + C_2H$	1.6×10^{6}	2.5	9.8	Estimated[o]	(75)
$OC_6H_4O + OH \leftrightharpoons H_2O + 2CO + C_2H_2 + C_2H$	4.4×10^{6}	2.0	1.4	Estimated[o]	(76)
Reactions of phenol molecules and derived radicals					
$C_6H_5OH \leftrightharpoons C_5H_6 + CO$	1.0×10^{12}	0.0	61.2	Horn [40]	(77)
$C_6H_5OH + O_2 \leftrightharpoons HO_2 + C_6H_5O$	1.0×10^{13}	0.0	38.8	Estimated[p]	(78)
$C_6H_5OH + O \leftrightharpoons OC_6H_4OH + H$	1.6×10^{13}	0.0	3.4	Estimated[q]	(79)
$C_6H_5OH + H \leftrightharpoons C_6H_5O + H_2$	1.2×10^{14}	0.0	12.4	Alzueta [7]	(80)
$C_6H_5OH + O \leftrightharpoons C_6H_5O + OH$	1.3×10^{13}	0.0	2.9	Alzueta [7]	(81)
$C_6H_5OH + OH \leftrightharpoons C_6H_5O + H_2O$	1.4×10^{8}	1.4	−0.96	Shandross [4]	(82)
$C_6H_5OH + HO_2 \leftrightharpoons C_6H_5O + H_2O_2$	1.0×10^{12}	0.0	10.0	Alzueta [7]	(83)
$C_6H_5OH + CH_3 \leftrightharpoons C_6H_5O + CH_4$	1.8×10^{11}	0.0	7.7	Mulcahy [41]	(84)
$C_6H_5OH + C_6H_5 \leftrightharpoons C_6H_5O + C_6H_6$	4.9×10^{12}	0.0	4.4	Alzueta [7]	(85)
$C_6H_5OH + C_5H_5 \leftrightharpoons C_6H_5O + C_5H_6$	4.9×10^{11}	0.0	9.4	Estimated[r]	(86)
$C_6H_5OH + a\text{-}C_3H_5 \leftrightharpoons C_6H_5O + C_3H_6$	4.9×10^{11}	0.0	9.4	Estimated[r]	(87)
$C_6H_5OH + i\text{-}C_4H_5 \leftrightharpoons C_6H_5O + 1,3\text{-}C_4H_6$	4.9×10^{11}	0.0	9.4	Estimated[r]	(88)
$C_6H_5OH + H \leftrightharpoons C_6H_4OH + H_2$	1.7×10^{14}	0.0	16.0	Shandross [4]	(89)
$C_6H_5OH + O \leftrightharpoons C_6H_4OH + OH$	2.0×10^{13}	0.0	14.7	Estimated[s]	(90)
$C_6H_5OH + OH \leftrightharpoons C_6H_4OH + H_2O$	1.4×10^{13}	0.0	4.6	Shandross [4]	(91)
$C_6H_5OH + HO_2 \leftrightharpoons C_6H_4OH + H_2O_2$	4.0×10^{11}	0.0	28.9	Estimated[s]	(92)
$C_6H_5OH + CH_3 \leftrightharpoons C_6H_4OH + CH_4$	2.0×10^{12}	0.0	15.0	Estimated[s]	(93)
$C_6H_4OH + O_2 \leftrightharpoons OC_6H_4OH + O$	2.1×10^{13}	0.0	6.1	Estimated[t]	(94)
$C_6H_4OH + H \leftrightharpoons C_6H_5OH$	1.0×10^{14}	0.0	0.0	Estimated[c]	(95)
Reactions of cyclopentadiene molecules and derived radicals					
$C_5H_6 + O_2 \leftrightharpoons C_5H_5 + HO_2$	1.4×10^{12}	0.0	31.6	Estimated[u]	(96)
$C_5H_6 + H \leftrightharpoons C_5H_7$	5.2×10^{13}	0.0	3.2	Estimated[o]	(97)
$C_5H_6 + O \leftrightharpoons C_5H_5O + H$	8.9×10^{12}	−0.15	0.59	Zhong [39]	(98)
$C_5H_6 + H{=}C_5H_5 + H_2$	2.8×10^{13}	0.0	2.0	Roy [42]	(99)
$C_5H_6 + O \leftrightharpoons C_5H_5 + OH$	4.8×10^{4}	2.7	1.1	Zhong [39]	(100)
$C_5H_6 + OH \leftrightharpoons C_5H_5 + H_2O$	3.1×10^{6}	2.0	0.0	Zhong [39]	(101)
$C_5H_6 + HO_2 \leftrightharpoons C_5H_5 + H_2O_2$	1.1×10^{4}	2.6	12.9	Zhong [39]	(102)
$C_5H_6 + CH_3 \leftrightharpoons C_5H_5 + CH_4$	1.8×10^{-1}	4.0	0.0	Zhong [39]	(103)
$C_5H_6 + a\text{-}C_3H_5 \leftrightharpoons C_5H_5 + C_3H_6$	6.0×10^{12}	0.0	0.0	Estimated[v]	(104)
$C_5H_6 + n\text{-}C_4H_5 \leftrightharpoons C_5H_5 + 1,3\text{-}C_4H_6$	6.0×10^{12}	0.0	0.0	Estimated[v]	(105)
$C_5H_6 + i\text{-}C_4H_5 \leftrightharpoons C_5H_5 + 1,3\text{-}C_4H_6$	6.0×10^{12}	0.0	0.0	Emdee [12]	(106)
$C_5H_7 \leftrightharpoons C_2H_2 + a\text{-}C_3H_5$	2.0×10^{13}	0.0	35.5	Estimated[w]	(107)
$C_5H_7 + O_2 \leftrightharpoons C_5H_6 + HO_2$	7.9×10^{11}	0.0	5.0	Estimated[x]	(108)
Reactions of cyclopentadione molecules and derived radicals					
$C_5H_4O \leftrightharpoons 2C_2H_2 + CO$	5.7×10^{32}	−6.76	68.5	Alzueta [7]	(109)
$C_5H_4O + H \leftrightharpoons CO + n\text{-}C_4H_5$	2.6×10^{13}	0.0	3.2	Estimated[o]	(110)
$C_5H_4O + O \leftrightharpoons C_4H_4 + CO_2$	1.0×10^{13}	0.0	2.0	Alzueta [7]	(111)
$C_5H_4O + H \leftrightharpoons C_5H_3O + H_2$	2.0×10^{12}	0.0	8.1	Alzueta [7]	(112)
$C_5H_4O + O \leftrightharpoons C_5H_3O + OH$	1.4×10^{13}	0.0	14.7	Alzueta [7]	(113)
$C_5H_4O + OH \leftrightharpoons C_5H_3O + H_2O$	1.1×10^{8}	1.42	1.45	Alzueta [7]	(114)
$C_5H_3O \leftrightharpoons C_2H_2 + CO + C_2H$	2.0×10^{13}	0.0	51.0	Estimated[y]	(115)
$C_5H_3O + O_2 \leftrightharpoons CO_2 + C_2H_2 + CHCO$	9.7×10^{58}	−13.47	38.2	Alzueta [7]	(116)

Continued

Table IV Continued

Reactions	A	n	E_a	References	Reaction No.
Reactions of cyclopentadienol molecules					
$C_5H_5OH + H \leftrightharpoons C_5H_5O + H_2$	4.0×10^{13}	0.0	6.1	Alzueta [7]	(117)
$C_5H_5OH + O \leftrightharpoons C_5H_5O + OH$	1.0×10^{13}	0.0	4.	Alzueta [7]	(118)
$C_5H_5OH + OH \leftrightharpoons C_5H_5O + H_2O$	1.0×10^{13}	0.0	1.7	Alzueta [7]	(119)
$C_5H_5OH + H \leftrightharpoons C_5H_4OH + H_2$	1.4×10^{13}	0.0	2.0	Estimated[z]	(120)
$C_5H_5OH + O \leftrightharpoons C_5H_4OH + OH$	4.8×10^{4}	2.7	1.1	Estimated[z]	(121)
$C_5H_5OH + OH \leftrightharpoons C_5H_4OH + H_2O$	1.5×10^{6}	2.0	0.0	Estimated[z]	(122)
Reactions of vinylketene molecules					
$C_4H_4O + H \leftrightharpoons C_2H_3 + CH_2CO$	1.3×10^{13}	0.0	3.0	Estimated[o]	(123)
$C_4H_4O + H \leftrightharpoons C_2H_4Z + CHCO$	1.3×10^{13}	0.0	3.0	Estimated[o]	(124)
$C_4H_4O + H \leftrightharpoons s\text{-}C_3H_5 + CO$	1.3×10^{13}	0.0	1.5	Estimated[o]	(125)
$C_4H_4O + OH \leftrightharpoons C_2H_3CHO + CHO$	1.4×10^{12}	0.0	−1.0	Estimated[o]	(126)
$C_4H_4O + OH \leftrightharpoons CO_2 + a\text{-}C_3H_5$	1.4×10^{12}	0.0	−1.0	Estimated[o]	(127)
$C_4H_4O + O \leftrightharpoons CH_2CHO + CHCO$	6.0×10^{4}	2.56	−1.1	Estimated[o]	(128)
$C_4H_4O + O \leftrightharpoons {}_2CH_2CO$	6.0×10^{4}	2.56	−1.1	Estimated[o]	(129)
$C_4H_4O + H \leftrightharpoons C_2H_2 + CHCO + H_2$	8.2×10^{5}	2.5	12.3	Estimated[o]	(130)
$C_4H_4O + H \leftrightharpoons C_3H_3 + CO + H_2$	4.1×10^{5}	2.5	9.8	Estimated[o]	(131)
$C_4H_4O + OH \leftrightharpoons C_2H_2 + CHCO + H_2O$	2.2×10^{6}	2.0	2.8	Estimated[o]	(132)
$C_4H_4O + OH \leftrightharpoons C_3H_3 + CO + H_2O$	1.1×10^{6}	2.0	1.5	Estimated[o]	(133)
$C_4H_4O + O \leftrightharpoons C_2H_2 + CHCO + OH$	1.2×10^{11}	0.7	8.7	Estimated[o]	(134)
$C_4H_4O + O \leftrightharpoons C_3H_3 + CO + OH$	6.0×10^{10}	0.7	8.7	Estimated[o]	(135)

Note. The rate constants are given at 1 atm ($k = A\,T^n \exp(-E_a/RT)$) in cc, mol, s, kcal units. Reference numbers are given in brackets when they appear for the first time. This mechanism should be used together with our C_0—C_6 reaction base [17].

[a] Rate constant taken equal to that of the H-abstraction with ethyl radicals with an activation energy 5 kcal mol^{-1} higher for resonance-stabilized radicals.

[b] Rate constant for the oxidation estimated using correlations proposed in the case of allylic radicals by Heyberger et al. [43].

[c] Rate constant taken equal to that of the recombination of ·H atoms with alkyl radicals as proposed by Allara and Shaw [44].

[d] Rate constant taken equal to that of the similar disproportionation of allyl radicals as proposed by Tsang [45].

[e] Estimated from the rate constants of the reverse addition reaction with an activation energy of 7 kcal mol^{-1} for the addition of ·C_2H or ·C_3H_3 radicals and of 3 kcal mol^{-1} for the addition of ·H atoms; A-factor is an average value for beta-scissions [43].

(l-C_6H_5 = ch///c/ch//ch/ch//ch., l-C_6H_4 = ch///c/ch//ch/c///ch, l-C_5H_5 = ch2(.)/ch//ch/c///ch).

[f] Rate constant taken equal to that of the addition of oxygen to alkyl radicals as proposed by Warth et al. [46].

[g] Values calculated using software KINGAS [47] based on thermochemical kinetics methods [26]. Activation energies of recombination are taken to be zero and A factors are estimated from modified collision theory [46].

[h] This reaction goes through an internal addition followed by beta-scissions involving the breaking of a C—C or a C—H bond. A-factor is an average value for beta-scissions [43] and activation energies have been adjusted to obtain a reactivity at low temperature, which is in agreement with the experimental results.

[i] Rate constant taken equal to that of the same reaction in the case of phenoxy radicals.

[j] Rate constant estimated from that of the same reaction in the case of allyl radicals [43].

[k] Rate constant for beta-scissions involving the breaking of a C—C or a C—H bond estimated by analogy with that of reactions (43) and (44).

[l] Rate parameters estimated from those proposed by Miyoshi et al. [48] and Alzueta et al. [7] (see text).

[m] Rate constant taken equal to that of the similar reaction in the case of cyclopentadienyl radicals.

[n] Rate constant taken equal to that of reaction (43).

[o] Rate constant for the addition of ·H atoms or the H-abstraction estimated using correlations proposed in the case of alkenes [43].

[p] A-factor taken from Alzueta et al. [7] and activation energy taken equal to the reaction enthalpy as proposed by Ingham et al. [49].

[q] Rate constant taken equal to that of the addition of ·O· atoms to toluene as proposed by Hoffmann et al. [50].

[r] Rate constant estimated from that of the H-abstraction with phenyl radicals, with A divided by 10 and an activation energy 5 kcal mol^{-1} higher to take into account the resonance stabilization of the involved radicals.

[s] Rate constant taken equal to that of the similar H-abstraction from benzene.

[t] Rate constant taken equal to that of the same reaction in the case of phenyl radicals.

[u] The rate constant of this bimolecular initiation with oxygen molecule has been calculated as proposed by Ingham et al. [49]: A is taken equal to $2 \times 7 \times 10^{12}$ cm^3 mol^{-1} s^{-1}, as there are two allylic hydrogen atoms abstractable and the activation energy to the reaction enthalpy.

[v] Rate constant taken equal to that of reaction (106).

[w] Rate constant for the beta-scission with the breaking of a C-C bond estimated using correlations proposed in the case of alkenyl radicals [43].

[x] Rate constant for the oxidation estimated using correlations proposed in the case of alkyl radicals proposed by Warth et al. [46].

[y] Rate constant taken equal to that of reaction (25).

[z] Rate constant taken equal to that of the same reaction in the case of cyclopentadiene molecules, with A-factor divided by 2 as only one H-atom is available.

order to be usable in all the temperature ranges studied, but are close to the values proposed by Braun-Unkoff et al. [33] at 1800 K, the temperature from which the flux of these reactions is no more negligible. We have not taken into account the formation of *o*-benzyne from phenyl radicals, which has been recently proposed based on theoretical calculations [53].

As proposed by Frank et al. [34], phenyl radicals can react with oxygen to form phenoxy radicals and ·O· atoms (27) or benzoquinone and H· atoms (28); according to Alzueta et al. [7], we have considered that reaction (28) leads mainly to *ortho*-benzoquinone. But to be able to reproduce our results at low temperature, we have also considered the formation of phenylperoxy radicals (29). The used rate parameters lead to a rate constant in agreement with the value measured by Yu and Lin [54] at 473 K. Other reactions of phenyl radicals include additions to acetylene (30) and benzene (31) molecules and termination steps with other radicals (32–42). It is worth noting that the formation of peroxy radicals is a reversible step and that the importance of the reverse reaction strongly depends on thermochemical data, which should then be calculated by a more accurate method than the groups additivity. In addition, the contributions of the three channels to the global reaction of phenyl radicals with oxygen depend on pressure. At high pressure, peroxy radicals can easily be stabilized, while at lower pressure, the formation of benzoquinone or phenoxy radicals are favored.

Very little is known about the reaction channels of phenylperoxy radicals. We have postulated that they can react by internal addition according to the following scheme:

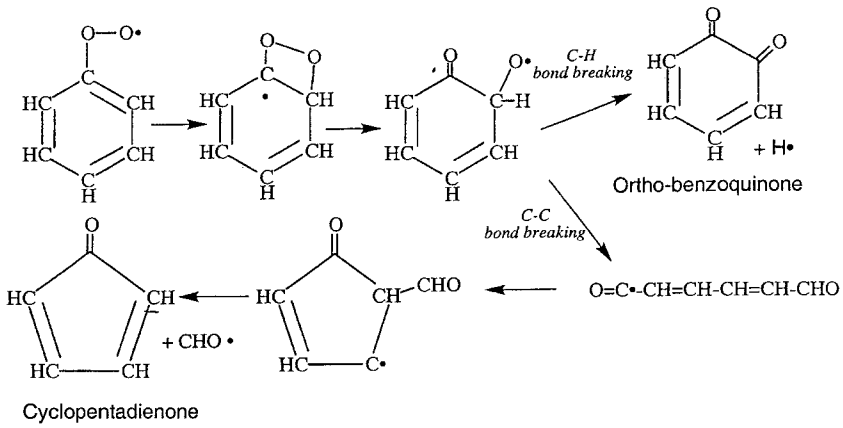

to form *ortho*-benzoquinone and H· atoms (43) or cyclopentadienone and CHO· radicals (44).

Resonance-stabilized phenoxy radicals can react either by the classical CO elimination to form cyclopentadienyl radicals (45) or by termination steps with other radicals (46–50). The reaction of phenoxy radicals with ·O· atoms has been experimentally studied at room temperature by Buth et al. [55], who have identified the formation of benzoquinone (49) and cyclopentadiene (50). Ab initio calculations of Lin and Mebel [38] have provided evidence for a possible third channel, involving the formation of hydroxyphenoxy radicals (48). In the case of these less abundant hydroxyphenoxy radicals, we have only considered the unimolecular CO elimination (51).

For the resonance cyclopentadienyl radicals, we have considered their linearization (52) as proposed by Braun-Unkoff et al. [33] and Burcat and Dvinyaninov [56], with reevaluated rate parameters for the following decompositions (53–54), the reaction with oxygen molecules (55), and termination steps with other radicals (56–62). The reactions with oxygen atoms and molecules are those proposed by Zhong and Bozzelli [39] in their theoretical study of the reactions of cyclopentadienyl radicals. The reactions of cyclopentadienyl radicals have also been studied by Roy et al. [42,57]. The $C_{10}H_{10}$ compound obtained by combination of two cyclopentadienyl radicals (61) is dihydrofulvalene. At low temperature, the direct reaction leading from two resonance-stabilized radicals to naphthalene and two reactive H atoms, as proposed by Roy et al. [42], would increase too much the reactivity of the system and cannot then be taken into account. The formation of naphthalene could only derive from an H-abstraction from dihydrofulvalene by small radicals, which are present in high concentration in flame.

The reactions of oxygenated C_5 cyclic radicals are not yet well defined. Cyclopentadienoxy radicals can decompose by beta-scission involving the breaking of a C—C (63) or a C—H bond (64) or combine with

H· atoms (65). Resonance-stabilized hydroxycyclopentadienyl radicals can react with oxygen molecules to form cyclopentadienone molecules (66) or by termination steps similar to those related to cyclopentadienyl radicals (67–71). The reaction of hydroxyalkyl radicals to form ketone molecules have been studied by Miyoshi et al. [48] who proposed an average rate constant, $k = 1 \times 10^{13}$ s^{-1} at 296 K. In the case of these cyclic resonance-stabilized hydroxy radicals, we have considered an activation energy of 10 kcal mol^{-1}.

Secondary Mechanism

The secondary mechanism includes the reactions of *ortho*-benzoquinone, phenol, cyclopentadiene, cyclopentadienone, and vinylketene molecules, which are produced in the primary mechanisms.

Ortho-benzoquinone can decompose to give cyclopentadienone and CO (72), as proposed by Frank et al. [34], or react by addition of H· atoms (74) or by H-abstractions with the subsequent decompositions of the obtained radicals (75–76) with rate constant derived from those proposed for alkenes [43].

Alzueta et al. [7] have experimentally studied and modeled the pyrolysis and oxidation of phenol in plug-flow conditions between 900 and 1450 K. For this compound, we have considered the molecular decomposition to give cyclopentadiene and carbon monoxide (77), the unimolecular initiation with oxygen molecules (78), the addition of ·O· atoms (79), and the H-abstractions, which can lead either to phenoxy radicals (80–88) or to C_6H_4·OH radicals (89–93). As the formation of the resonance-stabilized phenoxy radicals is easy, we have considered the H-abstraction from phenol with many radicals, including the main small resonance-stabilized radicals, i.e. cyclopentadienyl, allyl, and *i*-C_4H_5 radicals. C_6H_4·OH radicals can react with oxygen (94) in the same way as phenyl radical or combine with H· atoms (95).

Cyclopentadiene can react by unimolecular initiation with oxygen molecules (96), by additions of H· (97) and ·O· (98) atoms, and by H-abstractions to form cyclopentadienyl radicals (99–106). By analogy with the reaction of alkenyl radicals [40], the C_5H_7· radicals obtained by additions of H· atoms can react by beta–scission involving the breaking of a C—C bond (107) or by reaction with oxygen molecules to give back cyclopentadiene (108).

As proposed by Alzueta et al. [7], cyclopentadienone can react by molecular decomposition to give acetylene and carbon monoxide (109), by addition of ·O· (111) atoms and by H-abstractions to form cyclopentadienonyl radicals (112–114). But, we have also considered the addition of H· atoms to the double bonds of the ring and the following beta-scission involving the breaking of a C—C bond and the opening of the ring to form carbon monoxide and *n*-C_5H_5 radicals (110). Cyclopentadienonyl radicals can react with oxygen molecule (115) as proposed by Alzueta et al. [7], but we have also considered the decomposition by beta-scission involving the breaking of a C—C bond and the opening of the ring to form carbon monoxide, acetylene, and ·CHCO radicals (116).

Cyclopentadienol can react by H-abstractions to form either cyclopentadienoxy radicals (117–119) as proposed by Alzueta et al. [7] or the resonance-stabilized hydroxycyclopentadienyl radicals (120–122).

The reactions of vinylketene (CH_2=CHCH=C=O) were not considered in the C_0—C_6 reaction base [17]. They have been deduced from those of alkenes [43] and included the reactions of H· (123–125) and ·O· (128–129) atoms and of ·OH (126–127) radicals by addition to the double bonds or by H-abstraction (130–135).

In the case of the simulations in flame, secondary mechanisms of toluene, ethylbenzene, and styrene have been added. In the case of a flame, these secondary mechanisms had a small influence on the results, while this effect was negligible in other types of reactor, even in fuel-rich conditions, because very small amounts of toluene (formed by the reverse of reaction 34), ethylbenzene (formed by reaction 37), or styrene (formed by reaction 36) were formed. As our purpose was to investigate the chemistry of the oxidation of benzene and not the formation of PAHs, we have neglected the formation of aromatic compounds heavier than biphenyl and $C_6H_5C_3H_3$.

COMPARISON BETWEEN COMPUTED AND EXPERIMENTAL RESULTS

Simulations were performed using the softwares of CHEMKIN II [18]. We have tried to reproduce the experimental data described in this paper (jet-stirred reactor and shock tube), but to extend the validity of the proposed mechanism, we have also attempted to model results of the literature obtained in a flow tube [6] and in a near-sooting laminar flame [3]. The mechanism presented here before has been used for all the different performed simulations.

Perfectly Stirred Reactor

As the jet-stirred reactor has been proved to provide one of the very few types of gas-phase perfectly stirred reactor [58], we have modeld our results using the PSR

code of CHEMKIN II. Figures 2 and 3 display comparisons between the experimental (symbols) and computed (lines) results for the experiments performed in a jet-stirred reactor at Φ equal to 1.9 and 3.6, respectively. These figures show that our mechanism leads to an acceptable agreement for both equivalence ratios. The conversion of reactants are well reproduced in both cases, while the production of phenol is systematically overpredicted, whatever the residence time, betraying probably condensation problems for this compound before the entrance in the trap. For both equivalence ratios, the formation of carbon monoxide, carbon dioxide, methane, C_2 compounds, propyne, propene, and butadiene is overpredicted at short residence times, but the shape of the curves and the values at longer residence times are globally well reproduced. At 923 K, at an equivalence ratio of 1.9, and at a residence time of 4 s, C_2 compounds contain 53% acetylene and 47% ethylene.

Shock Tube

Computed results for the shock tube appear in Fig. 4. It is worth noting that the experimental OH emission at 306 nm is related to electronically exited OH concentration and is not directly proportional to OH radical concentration. Nevertheless, previous work [18] has shown a correct agreement between the shapes of the profiles of experimental emission and calculated OH concentration during the rise of the signal, which is the important part of the curve for the determination of ignition delays. Both experimentally and theoretically, the ignition delay is determined at 10% of the maximum OH peak. Model results reproduce the systematic trends of the measurements, including variations in ignition delays with temperature, equivalence ratio, and concentration of benzene. Agreement deteriorates slightly for Φ equal to 0.5, where computed delay times are about two times higher than the experimental values. At Φ equal to 1 and 1.25% of benzene, the computed line is closer to the experimental results presented in this paper than to the line derived from the correlation proposed by Burcat et al. [5].

Flow Reactor

Lovell et al. [6] have studied the oxidation of benzene in a flow reactor at 1100 K, atmospheric pressure, with nitrogen as bath gas, for a concentration of benzene of 1580 ppm and for three equivalence ratios, 0.76, 1, and 3. Figures 5 and 6 display comparisons between the experimental (symbols) and computed (lines) results at Φ equal to 0.76 and 1.3, respectively, and show that a globally correct agreement can be observed in both cases. For the shortness of the paper, simulations at Φ equal to 1 are not presented, but they lead to a similar agreement. The model can satisfactorily reproduce the consumption of benzene and the formation of phenol, cyclopentadiene, and C_4 compounds (99% vinylacetylene and 0.9% 1,3-butadiene, at Φ equal to 0.76, at a residence time of 0.075 s) in both conditions. The production of carbon monoxide is well simulated at Φ equal to 0.76, while it is overestimated by a factor 2 for the longest residence times at Φ equal to 1.3. The formation of C_2 compounds (8% acetylene and 92% ethylene, at Φ equal to 0.76, at a residence time of 0.075 s) is slightly underpredicted at Φ equal to 0.76, while it is overpredicted by a factor up to 3 at Φ equal to 1.3.

Our model allows us to obtain better predictions than the mechanisms proposed by Emdee et al. [12], especially for the production of carbon monoxide, reflecting the fact that we have a more detailed submechanism for

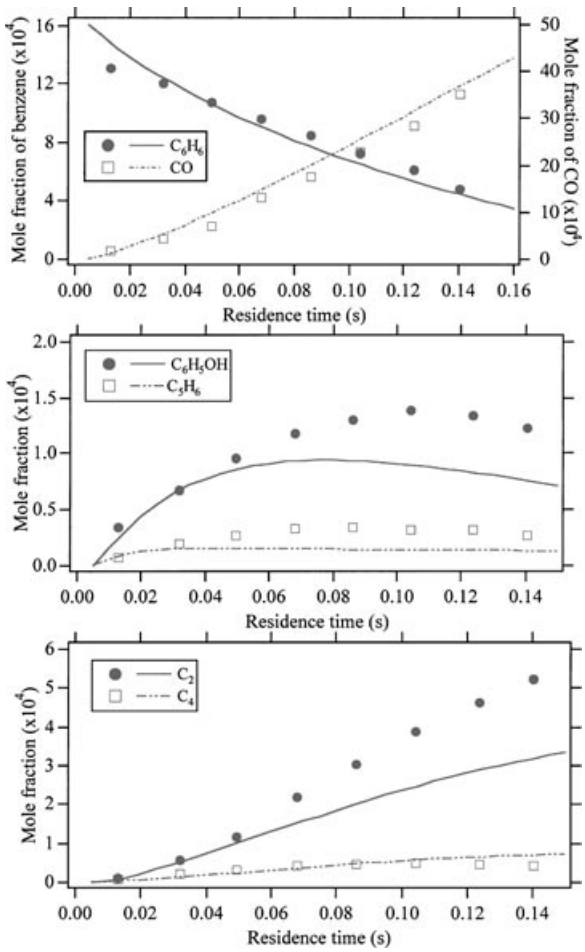

Figure 5 Oxidation of benzene in flow reactor at 1100 K [6]. Comparison between experimental (symbols) and computed (lines) species vs. residence time at Φ = 0.76.

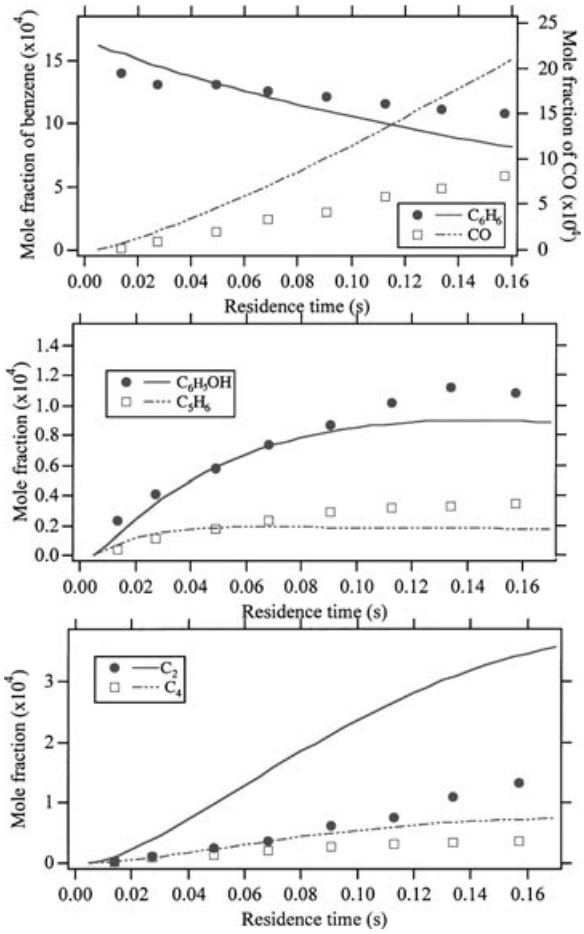

Figure 6 Oxidation of benzene in flow reactor at 1100 K [6]. Comparison between experimental (symbols) and computed (lines) species vs. residence time at $\Phi = 1.3$.

C_5 species. It is worth noting that in our case no time shift has been necessary. These data have been also modeled by Zhong and Bozzelli [39] in order to test their submechanism for the oxidation of cyclopentadiene. In all the studied conditions, their agreement for the profiles of benzene and carbon monoxide is good, but they overpredict the formation of cyclopentadiene by a factor 2, even for short residence times, and they do not present the formation of phenol, C_2, and C_4 compounds. An example of simulation of these experiments in lean mixture is presented by Alzueta et al. [7], but the agreement is much poorer than what can be obtained by Zhong and Bozzelli [39] and than what is shown here.

Premixed Flame

Bittner and Howard [3] have studied a near-sooting laminar premixed benzene–oxygen–argon flame stabilized on a burner at 2.67 kPa and analyzed by using a molecular beam mass spectrometer system. They have used mixtures containing 13.5% of benzene at an equivalence ratio of 1.8 and a cold gas velocity of 0.5 m s^{-1} at room temperature.

To model correctly a laminar premixed flame, it is necessary to consider the transport of species, momentum and energy, in a multicomponent gaseous mixture. CHEMKIN II [20] takes into account these phenomena by means of multicomponent transport properties (diffusion coefficients, viscosities, and thermal diffusion coefficients). These coefficients are calculated using relations involving the ratio ε/k_B (with ε the Lennard–Jones well depth and k_B the Boltzmann constant), the Lennard–Jones collision diameter σ, the dipole moment μ, and the polarizability α. A file containing these parameters for several simple species is provided in the CHEMKIN II package [20]. However, in the case of the oxidation of benzene, it has been necessary to estimate transport data, especially the Lennard–Jones parameters (ε/k_B and σ), for large molecules. For this, we used correlations found in the literature [59]:

$$\sigma^3 P_c/T_c = 13.56 + 9.6\omega + 6.26\omega^2 - 10\omega^3$$

$$(\varepsilon/k_B)/T_c = 0.753 - 0.468\omega - 0.277\omega^2 + 0.426\omega^3$$

where P_c (atm), T_c (K), and ω represent, respectively, the critical pressure, the critical temperature, and the acentric factor. These last parameters can be found in the literature for a large range of molecules or can be estimated by means of the Joback group contributions [60]. Table V summarizes, for several molecules involved in the oxidation of benzene, the overall parameters used in the calculation of Lennard–Jones parameters. The coefficients of the molecule, which has the closest chemical structure, were used for radicals.

Figure 7 presents a comparison between these experimental data (symbols) and the predictions (lines) given by our model. The major stable species, benzene, oxygen, carbon monoxide, carbon dioxide, acetylene, phenol, cyclopentadiene, hydrogen, and water, are well predicted, while the maximum of vinylacetylene is underpredicted. The profiles of H· and ·OH radicals are well represented, but those of ·HO_2 (up to factor 2) and phenyl (up to factor 4) radicals are overestimated. The agreement obtained here is globally similar to that of other recent modeling work [9,13–15].

ANALYSIS OF THE MECHANISM

It is worth noting that the fluxes and sensitivity analyses presented hereafter have been performed with the

Table V Critical Temperature and Pressure, Acentric Factor, and Lennard–Jones Parameters

Species	Critical Temperature T_c (K)	Critical Pressure P_c (atm)	Acentric Factor ω	ε/k_b (K)	σ (A)
C_6H_6	561.9	48.6	0.216	361.5	5.7
OC_6H_4O	746	60	0.486	379.7	6.1
C_6H_5OH	694.1	60.5	0.439	368.0	5.9
Toluene	593.8	41.6	0.258	368.8	6.1
$C_6H_5C_2H$	650	44	0.237	410.9	6.2
Ethylbenzene	616.9	36.9	0.32	363.3	6.6
Styrene	647.4	39.4	0.243	407.2	6.4
Biphenyl	768	31.8	0.416	415.5	7.6
l-C_5H_6	493	44.6	0.174	328.1	5.5
C_5H_6	532	49.3	0.2	346.7	5.5
$C_{10}H_{10}$	687	54.5	0.448	361.4	6.1
C_5H_4O	625	52	0.298	375.1	5.9
C_5H_5OH	612.8	54.6	0.614	281.8	6.0
C_4H_4O	445	55.7	0.286	269.9	5.1

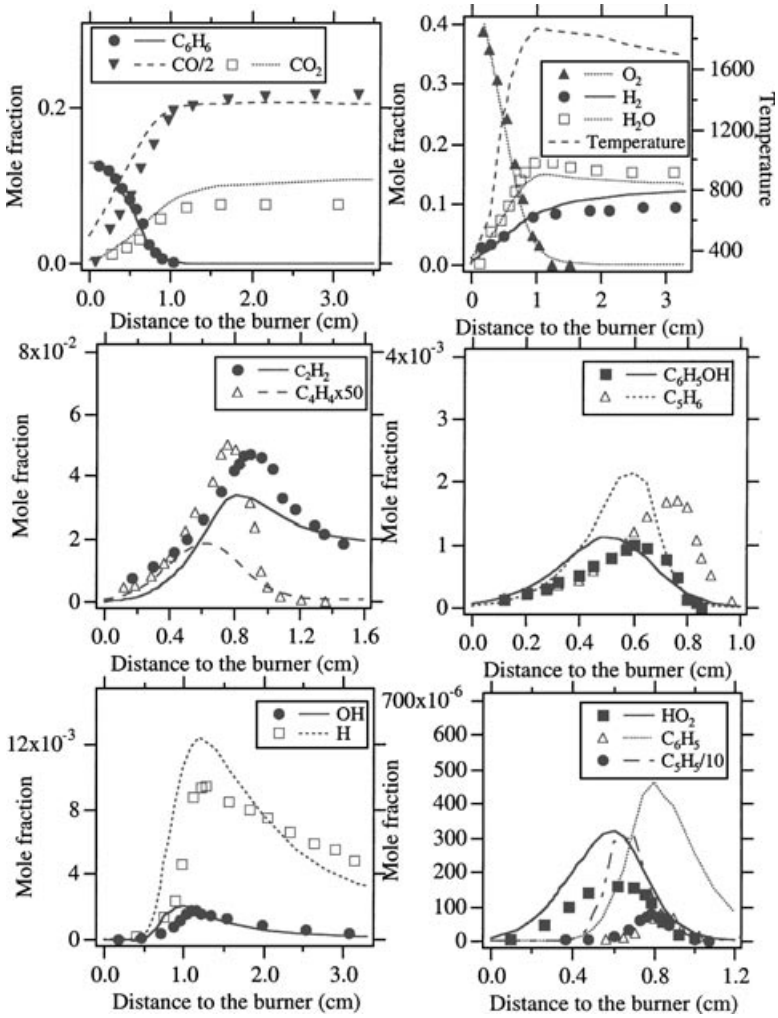

Figure 7 Near-sooting laminar premixed flame of benzene [3]. Comparison between experimental (symbols) and computed (lines) species vs. distance to the burner at $\Phi = 1.8$.

mechanism described previously and that the accuracy of conclusions derived from them can only reflect the accuracy of the proposed reaction channels and of the used thermodynamic and kinetic data.

Figures 8 and 9a present fluxes and sensitivity analysis computed in a jet-stirred reactor at 923 K, an equivalence ratio of 1.9, and a residence time of 4 s corresponding to a 30% conversion of benzene. Figure 9b presents a sensitivity analysis computed around 1300 K and a shock tube at 70% conversion of benzene. Figure 8b demonstrates the determinant role for ignition delays of termination (e.g., the recombinations of ·H atoms with phenoxy or cyclopentadienyl radicals) and branching (e.g., the branching reaction between ·H atoms and oxygen molecules) reactions. Figures 10 and 11 display fluxes computed in a flow tube at 1100 K (equivalence ratio of 0.76, residence time of 0.075 s corresponding to a 47% conversion of benzene) and in a laminar flame at 1710 K (equivalence ratio of 1.8, distance to the burner of 0.75 cm corresponding to a 85% conversion of benzene), respectively.

Main Reaction Pathways of Benzene Molecules

In all cases, benzene reacts mainly by two channels, addition of ·O· atoms to give phenoxy radicals (4) and metatheses, i.e. H-abstraction by H· atoms, OH·, and phenoxy radicals, to form phenyl radicals (8, 10, −85). In a perfectly stirred reactor, at 923 K, metatheses account for 66% of the benzene consumption, while 32% is due to the addition of ·O· atoms. The ratio between these two channels does not depend much on temperature or equivalence ratio. Above 1800 K and in a flame, benzene slightly decomposes to propargyl radicals (reaction of the C_0—C_6 reaction base [19]).

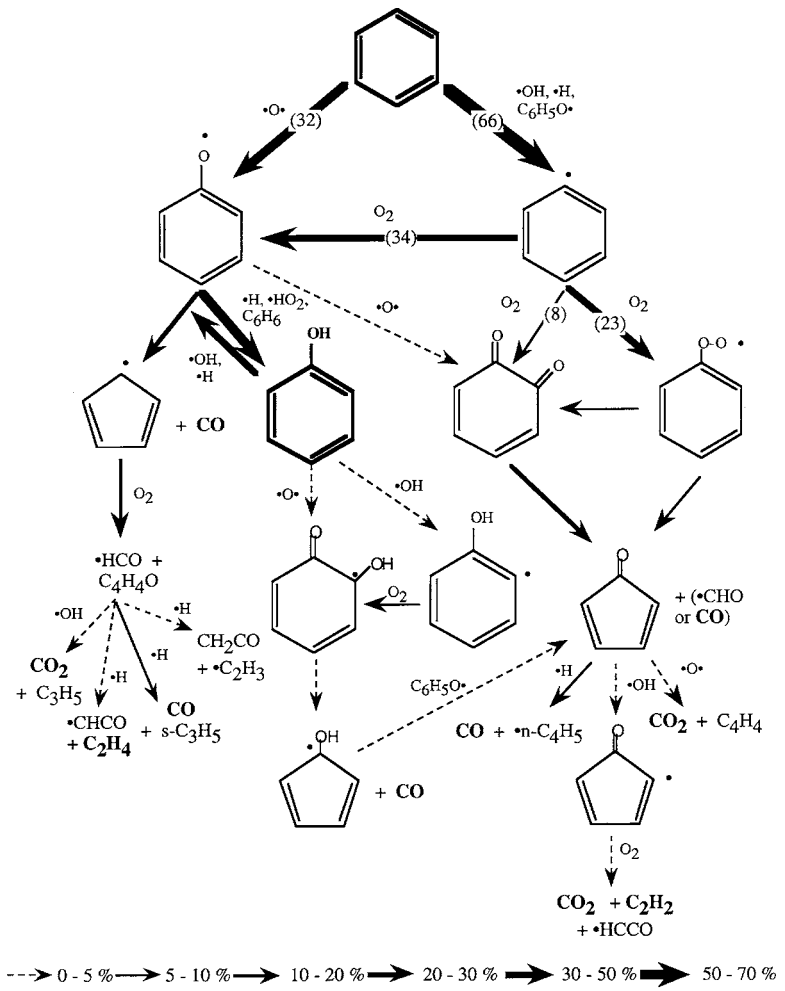

Figure 8 Oxidation of benzene in a jet-stirred reactor at 923 K. Flux analysis at $\Phi = 1.9$ for a residence time of 4 s.

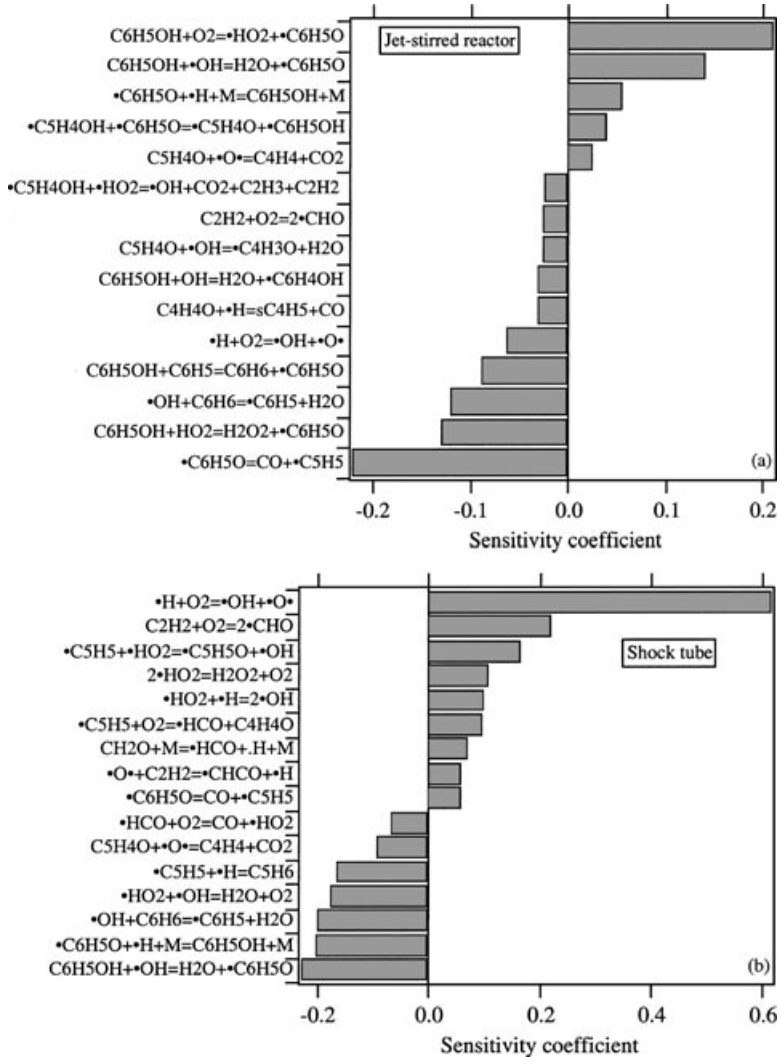

Figure 9 Oxidation of benzene in a jet-stirred reactor and in a shock tube. Sensitivity analyses related to (a) the conversion of benzene in a jet-stirred reactor, at 923 K, $\Phi = 1.9$ and a residence time of 4 s (only reactions, with an absolute value of the sensitivity coefficient above 0.024, are shown) and to (b) the mole fraction of hydroxyl radicals in a shock tube at an initial temperature of 1300 K, at $\Phi = 1$ and a residence time corresponding to 50% conversion of benzene (only reactions, with an absolute value of the sensitivity coefficient above 0.06, are shown).

Reactions Deriving from the Formation of Phenoxy Radicals

Phenoxy radicals can react with ·H atoms (46) or, at low temperature, with $\cdot HO_2$ radicals (−78) or benzene molecules (−85), to form phenol or eliminate carbon monoxide (45) to give cyclopentadienyl radicals. A minor channel involves the formation of benzoquinone by addition of ·O· atoms (49). The importance of the CO elimination increases with temperature, while that of termination steps decreases. Figure 9 shows that the reactions forming or consuming resonance-stabilized phenoxy radicals have important sensitivity coefficients in a jet-stirred reactor and in a shock tube. It is worth noting that the rate constants of some important reactions of phenoxy radicals, such as their reactions with $\cdot HO_2$ radicals (−78) or the disproportionation with hydroxycyclopentadienyl radicals (51), are only based on estimations.

The abstractions of the hydroxylic H-atoms by H· (80) and ·O· (81) atoms, OH· (82), and, at low temperature, $\cdot HO_2$ radicals (83) to give back phenoxy radical are important reactions of phenol. In a perfectly stirred reactor, at 923 K, these reactions account for 80% of the phenol consumption. This is due to the fact that phenoxy radicals are resonance-stabilized. At 1710 K, the major reaction is the molecular decompositions to

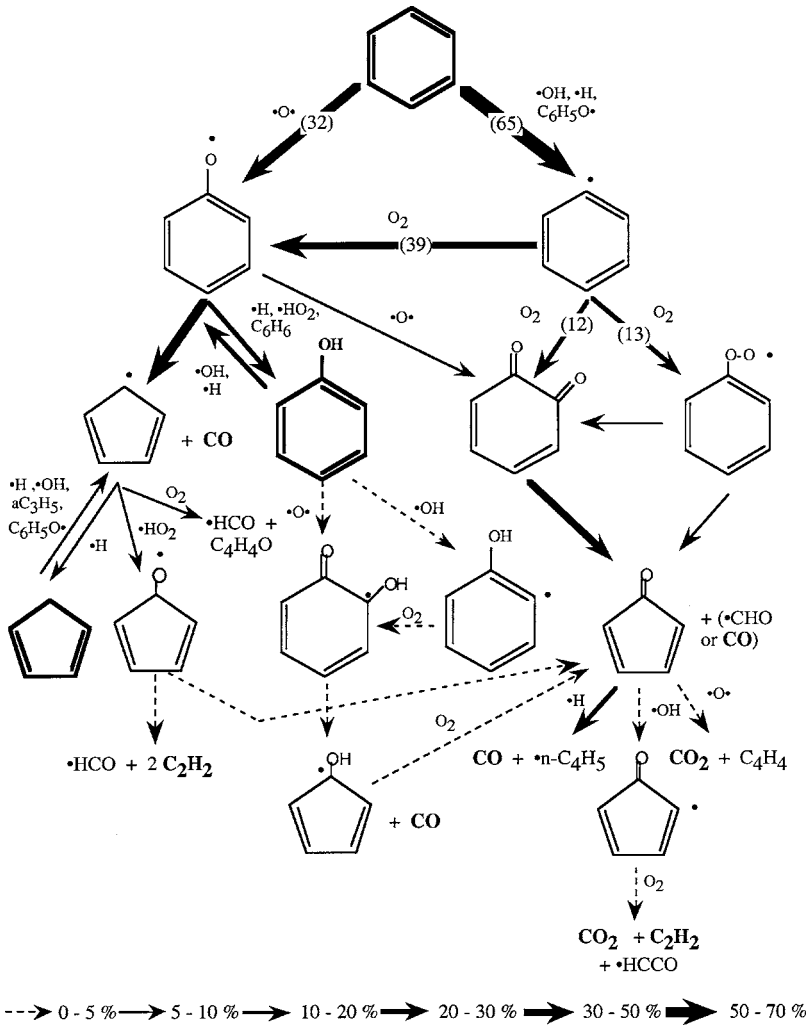

Figure 10 Oxidation of benzene in flow reactor at 1100 K. Flux analysis at $\Phi = 0.76$ at a residence time of 0.075 s.

give cyclopentadiene and carbon monoxide (77). Other reactions include the addition of ·O· atoms to form hydroxyphenoxy radicals (79) and the abstraction of aromatic H-atoms by OH· radicals to give $\cdot C_6H_4OH$ radicals (91), which react rapidly with oxygen molecules to give hydroxyphenoxy radicals (94). Hydroxyphenoxy radicals decompose by CO elimination to give the resonance-stabilized hydroxycyclopentadienyl radicals (51), which react mainly by disproportionation with phenoxy radicals and lead to cyclopentadienone (71).

Reactions Deriving from the Formation of Phenyl Radicals

In the studied conditions, phenyl radicals react mainly with oxygen molecules. In perfectly stirred and flow reactors (below 1100 K), the three considered channels, the branching step to give ·O· atoms and phenoxy radicals (27), the formation of ·H atoms and of benzoquinone (28), and the production of phenylperoxy radicals, are of importance (29). Of course, the formation of phenylperoxy radicals decreases with temperature. Phenylperoxy radicals decompose to give either ·H atoms or benzoquinone (43) or ·HCO radicals and cyclopentadienone (44). Cyclopentadienone is also the main product of the decomposition of benzoquinone by CO elimination (72).

Above 1800 K and in a low-pressure flame, a small fraction of phenyl radicals decompose to give acetylene and n-$C_4H_3\cdot$ radicals (reaction of the C_0—C_6 reaction base [19]) or are linearized (24) and decomposed to produce also acetylene and n-$C_4H_3\cdot$ radicals (25).

Reactions of C_5 Compounds

In a perfectly stirred reactor, at 923 K and for an equivalence ratio equal to 1.9, the main reaction of

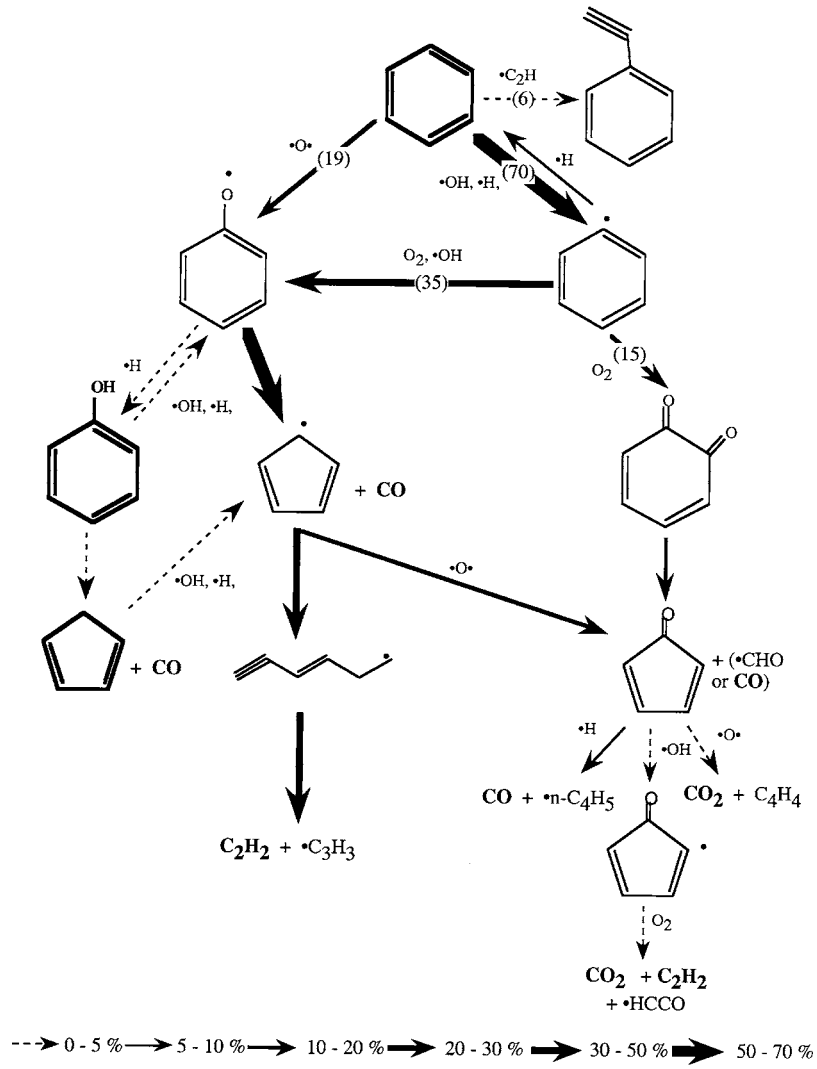

Figure 11 Near-sooting laminar premixed flame of benzene. Flux analysis at $\Phi = 1.8$, a distance to the burner equal to 0.75 cm, and a temperature of 1710 K.

cyclopentadienyl radicals is with oxygen to produce ·HCO radicals and vinylketene (55). The four main reactions of vinylketene are with ·H atoms to produce CH_2CO and vinyl radicals (123), ethylene and ·CHCO radicals (124), or carbon monoxide and *s*-C_3H_5 radicals (125), and with ·OH radicals to give carbon dioxide and allyl radical (127). The decomposition of *s*-C_3H_5 radicals by breaking of a C—H bond leads to the formation of propyne (reaction of the C_0—C_6 reaction base [19]). The reaction of allyl radicals with phenol explains the major part of the production of propene (87).

In a flow reactor and in a shock tube, other reactions of cyclopentadienyl radicals include the formation of cyclopentadiene by combination with ·H atoms (56) and that of ·OH and cyclopentadienoxy radicals by combination with $\cdot HO_2$ radicals (60). The major reaction of cyclopentadienyl radicals in a flame is its linearization (52) and the decomposition of the linear isomer to give acetylene and propargyl radicals (54). Figure 9b shows the important role of resonance-stabilized cyclopentadienyl radicals for ignition delays. The rate constants of most reactions of cyclopentadienyl radicals are based on calculations or estimations. The very few direct measurements of rate constants for these radicals have been obtained at high temperature in a shock tube [33,57].

Cyclopentadiene reacts mainly by metatheses with ·H atoms (99) and ·OH (101), and allyl (104) and phenoxy (−86) radicals to give back cyclopentadienyl radicals. The major reactions of cyclopentadienoxy radicals are decompositions to give ·HCO radicals and acetylene (63) and ·H atoms and cyclopentadienone (64).

Cyclopentadienone reacts mainly with ·H atoms to produce *n*-C_4H_5· and carbon monoxide (110). The reaction of *n*-C_4H_5· radicals with oxygen leads to vinylacetylene (110), which can react with ·H atoms to give *i*-C_4H_5· radicals (reactions of the C_0–C_6 reaction base [19]), which can react with phenol to produce 1,3-butadiene (88). Other reactions of cyclopentadienone include the reaction with ·O· atoms to give vinylacetylene and carbon dioxide (111) and the H-abstraction with ·OH radicals to produce cyclopentadienonyl radicals (114), which react with oxygen molecules and lead to ·HCCO radicals, carbon dioxide, and acetylene (116).

It is worth noting that, in all the studied conditions, the reactions of oxygenated C_5 cyclic radicals, which are not yet well defined, are important stages to explain the formation of small degradation products such as carbon monoxide and C_2 and C_4 compounds. That could explain the problems encountered in our simulations to reproduce some of these light compounds.

CONCLUSION

This work has allowed us to present new experimental results for the oxidation of benzene in a jet-stirred reactor at a temperature of 923 K and in a shock tube at temperatures between 1230 and 1970 K and to propose a detailed mechanism able to reproduce these data, but also previously published experiments in a flow reactor and in a near-sooting laminar flame [3,6].

The reactions of importance in this mechanism have been determined by using flux and sensitivity analyses. Amongst them, the reactions of oxygenated C_5 cyclic radicals are yet very uncertain and are a necessary subject of studies for specialists of elementary reactions to progress toward a better modeling of the oxidation of aromatic compounds.

Despite these uncertainties in the chemistry of C_5 compounds, the mechanism proposed here constitutes a first basis in the further development of models for the oxidation of other aromatic compounds, such as toluene or xylene.

BIBLIOGRAPHY

1. Walker, R. W.; Morley, C. In Comprehensive Chemical Kinetics; Pilling, M. J. (Ed.); Elsevier: Amsterdam, 1997; p. 1.
2. Guibet, J. C. Fuels and Engines; Publications de l'Institut Français du Pétrole, Editions Technip, 1999; Vols. 1 and 2.
3. Bittner, J. D.; Howard, J. B. Symp (Int) Combust, [Proc] 1981, 8, 1105.
4. Shandross, R. A.; Longwell, J. P.; Howard, J. B. Int Combust Proc 1996, 26, 711.
5. Burcat, A.; Snyder, C.; Brabbs, T. NASA TM-87312, 1986.
6. Lovell, A. B.; Brezinsky, K.; Glassman, I. Symp (Int) Combust, [Proc] 1988, 22, 1063.
7. Alzueta, M. U.; Glarborg, P.; Dam-Johansen, K. Int J Chem Kinet 2000, 32, 498.
8. Chai, Y.; Pfefferle, L. D. Fuel 1998, 77, 313.
9. Ristori, A.; Dagaut, P.; El Bakali, A.; Pengloan, G.; Cathonnet, M. Combust Sci Technol 2001, 167, 223.
10. Schöbel, A.; Glass, A.G.; Krebs, L.; Braun-Unkhoff, M.; Wahl, C.; Frank, P. Chemosphere 2001, 42, 591.
11. Bittker, D. A. Combust Sci Technol 1991, 79, 49.
12. Emdee, J. L.; Brezinsky, K.; Glassman, I. J Phys Chem 1992, 96, 2151.
13. Lindstedt, R. P.; Skevis, G. Combust Flame 1994, 99, 551.
14. Zhang, H. Y.; McKinnon, J. T. Combust Sci Technol 1995, 107, 261.
15. Tan, Y.; Frank, P. Symp (Int) Combust, [Proc] 1996, 26, 677.
16. Richter, H.; Grieco, W. J.; Howard, J. Combust Flame 1999, 119, 1.
17. Baugé, J. C.; Battin-Leclerc, F.; Baronnet, F. Int J Chem Kinet 1998, 30, 629.
18. Fournet, R.; Baugé, J. C.; Battin-Leclerc, F. Int J Chem Kinet 1999, 31, 361.
19. Belmekki, N.; Glaude, P. A.; Da Costa, I.; Fournet, R.; Battin-Leclerc, F. Int J Chem Kinet 2002, 34, 172.
20. Kee, R. J.; Rupley, F. M.; Miller, J. A. Sandia Laboratories Report, SAND 89-8009B, 1993.
21. Barbé, P.; Battin-Leclerc, F.; Côme, G. M. J Chim Phys 1995, 92, 1666.
22. Baulch, D. L.; Cobos, C. J.; Cox, R. A.; Frank, P.; Hayman, G. D.; Just, T.; Kerr, J. A.; Murrells, T. P.; Pilling, M. J.; Troe, J.; Walker, R. W.; Warnatz, J. Combust Flame 1994, 98, 59.
23. Tsang, W.; Hampson, R. F. J Phys Chem Ref Data 1986, 15, 1087.
24. Troe, J. Ber Bunsen-Ges Phys Chem 1974, 78, 478.
25. Muller, C.; Michel, V.; Scacchi, G.; Côme, G. M. J Chim Phys 1995, 92, 1154.
26. Benson, S. W. Thermochemical Kinetics, 2nd ed.; Wiley: New York, 1976.
27. Wang, H.; Frenklach, M. Combust Flame 1994, 110, 173.
28. Mebel, A. M.; Lin, M. C.; Yu, T.; Yorokuma, K. J Phys Chem A 1997, 101, 3189.
29. Nicovich, J. M.; Gump, C.; Ravishankara, A. R. J Phys Chem 1982, 86, 1684.
30. Baulch, D. L.; Cobos, C. J.; Cox, R. A.; Esser, C.; Frank, P.; Just, T.; Kerr, J. A.; Pilling, M. J.; Troe, J.; Walker, R. W.; Warnatz, J. J Phys Chem Ref Data 1992, 21, 411.
31. Zhang, H. X.; Ahonkhai, S. I.; Back, M. H. Can J Chem 1989, 67, 1541.

32. Weissman, M.; Benson, S. W. Prog Energy Combust Sci 1989, 15, 273.
33. Braun-Unkhoff, M.; Frank, P.; Just, Th. Symp (Int) Combust, [Proc] 1988, 22, 1023.
34. Frank, P.; Herzler, J.; Just, Th.; Wahl, C. Symp (Int) Combust, [Proc] 1994, 25, 833.
35. Marinov, M. N.; Pitz, W. J.; Westbrook, C. K.; Castaldi, M. J.; Senkan, S. M. Combust Sci Technol 1996, 116, 211.
36. Colket, M. B.; Seery, D. J. Symp (Int) Combust, [Proc] 1994, 25, 883.
37. D'Anna, A.; Violi, A. Symp (Int) Combust, [Proc] 1998, 27, 425.
38. Lin, M. C.; Mebel, A. M. M. J Phys Org Chem 1995, 8, 407.
39. Zhong, X.; Bozzelli, J. W. J Phys Chem A 1998, 102, 3537.
40. Horn, C.; Roy, K.; Frank, P.; Slutsky, V. G.; Just, Th. Int Combust Proc 1998, 27, 321.
41. Mulcahy, M. F. R.; Williams, D. J. Aust J Chem 1965, 18, 20.
42. Roy, K.; Horn, C.; Frank, P.; Just, Th. Int Combust Proc 1998, 27, 329.
43. Heyberger, B.; Belmekki, N.; Conraud, V.; Glaude, P. A.; Fournet, R.; Battin-Leclerc, F. Int J Chem Kinet 2002, 34, 172.
44. Allara, D. L.; Shaw, R. J Phys Chem Ref Data 1980, 9, 3.
45. Tsang, W. J Phys Chem Ref Data 1991, 20, 221.
46. Warth, V.; Stef, N.; Glaude, P. A.; Battin-Leclerc, F.; Scacchi, G.; Côme, G. M. Combust Flame 1998, 114, 81.
47. Bloch-Michel, V. PhD Thesis, Institut National Polytechnique de Lorraine, Nancy, France, 1995.
48. Miyoshi, A.; Matsui, H.; Washida, N. J Phys Chem 1990, 94, 3016.
49. Ingham, T.; Walker, R. W.; Woolford, R. E. Symp (Int) Combust, [Proc] 1994, 25, 767.
50. Hoffmann, A.; Klatt, M.; Wagner, H. Gg. Z Chem Phys (Neue Folge) 1990, 168, 1.
51. Scherer, S.; Just, Th.; Frank, P. Symp (Int) Combust, [Proc] 2000, 28, 1511.
52. Stein, S. E.; Walker, J. A.; Suryan, M. M.; Fahr, A. Int Combust Proc 1990, 23, 85.
53. Wang, H.; Laskin, A.; Moriarty, N. W.; Frenklach, M. Int Combust Proc 2000, 28, 1545.
54. Yu, T.; Lin, M. C. J Am Chem Soc 1994, 85, 2262.
55. Buth, R.; Hoyermann, K.; Seeba, J. Symp (Int) Combust, [Proc] 1994, 25, 841.
56. Burcat, A.; Dvinyaninov, M. Int J Chem Kinet 1996, 29, 505.
57. Roy, K.; Braun-Unkhoff, M.; Frank, P.; Just, Th. Int J Chem Kinet 2001, 33, 821.
58. Matras, D.; Villermaux, J. Chem Eng Sci 1973, 28, 129.
59. Gosse, J. Techniques de l'ingénieur K 1991, 425, 1.
60. Reid, R. C.; Prausnitz, J. M.; Poling, B. E. The Properties of Gases and Liquids, 4th ed.; McGraw-Hill: New York, 1987.